Synthesis by nitroxide-mediated aqueous dispersion polymerization, characterization, and physical core-crosslinking of pH- and thermoresponsive dynamic diblock copolymer micelles

Guillaume Delaittre, Maud Save, Marianne Gaborieau, Patrice Castignolles, Jutta Rieger, Bernadette Charleux

Synthesis by Nitroxide-Mediated Aqueous Dispersion Polymerization, Characterization, and Physical Core-Crosslinking of pH- and Thermoresponsive Dynamic Diblock Copolymer Micelles

Guillaume Delaittre,[*,†] *Maud Save,*[‡] *Marianne Gaborieau,*[¤] *Patrice Castignolles,*[¶] *Jutta Rieger,*[§] *Bernadette Charleux**[*,¥]

† Preparative Macromolecular Chemistry, Institut für Technische Chemie und Polymerchemie, Karlsruhe Institute of Technology (KIT), Engesserstr.18, 76128 Karlsruhe, Germany.

‡ IPREM Equipe de Physique et Chimie des Polymères, UMR 5254 CNRS, Université de Pau et des Pays de L'Adour, Hélioparc, 2 Avenue du Président Angot, 64053 Pau Cedex, France.

¤ University of Western Sydney, Nanoscale Organisation and Dynamics Group, School of Science and Health, Parramatta Campus, Locked Bag 1797, Penrith NSW 2751, Australia

¶ University of Western Sydney, School Science and Health, Australian Centre for Research on Separation Science (ACROSS), Parramatta Campus, Locked Bag 1797, Penrith NSW 2751, Australia.

§ UPMC Univ. Paris 6, Sorbonne Universités and CNRS, Laboratoire de Chimie des Polymères (LCP), UMR 7610, 3 rue Galilée, 94200 Ivry, France.

¥ Université de Lyon, Univ Lyon 1, CPE Lyon, CNRS, UMR 5265, C2P2 (Chemistry, Catalysis, Polymers & Processes), Team LCPP Bat 308F, 43 Bd du 11 novembre 1918, 69616 Villeurbanne, France.

* *Corresponding authors:* guillaume.delaittre@kit.edu, bernadette.charleux@lcpp.cpe.fr

RECEIVED DATE (to be automatically inserted after your manuscript is accepted if required according to the journal that you are submitting your paper to)

TITLE RUNNING HEAD. Dynamic Stimuli-Sensitive Micelles Synthesized by Aqueous Dispersion NMP

ABSTRACT. Diblock copolymers consisting of a poly(sodium acrylate) (PAA) segment and LCST-type poly(*N*,*N*-diethylacrylamide) (PDEAAm) block were obtained by nitroxide-mediated

polymerization in aqueous dispersion using a water-soluble macroalkoxyamine. The influence of several parameters on the polymerization (temperature, initial free nitroxide or macroalkoxyamine concentrations, and solids content) was evaluated in terms of kinetics, macromolecular control, and colloidal features. As determined by dynamic light scattering (DLS), stable dispersions of monodisperse particles could be obtained for solids content as high as 39 wt% without the need for any additional surfactant via a *polymerization-induced self-assembly* mechanism. Rendered possible by the use of a controlled/living polymerization process, the effective semi-batch incorporation of hydrophobic units (styrene) in the growing chains during the polymerization allowed the formation of physically crosslinked nanogels. The pH- and temperature-sensitivity were proved by means of DLS and high-sensitivity differential scanning calorimetry (HSDSC) measurements. Due to the formation of aggregates observed by size-exclusion chromatography in *N*,*N*-dimethylformamide, accurate molar masses could not be determined directly but deconvoluted hydrodynamic volume distributions suggested a good control of the polymerization.

KEYWORDS. controlled/living radical polymerization, nanogels, hydrodynamic volume distribution, core-shell, physical crosslinking

Introduction

Nitroxide-mediated polymerization (NMP)[1] is one of the main techniques in the field of reversible-deactivation radical polymerization (also commonly called controlled radical polymerization, CRP).[2] Similarly to the other principal techniques, namely atom transfer radical polymerization (ATRP)[3] and reversible addition-fragmentation transfer polymerization (RAFT),[4] it allows one to obtain well-defined homopolymers (predictable molar masses and low polydispersity indices) able to react with a new batch of monomer to produce block copolymers. Compared to ATRP or RAFT, NMP presents the advantage of using a very simple system as it requires the use of a single component, an alkoxyamine playing the dual role of initiator and controlling agent. Furthermore the most common nitroxides or alkoxyamines based on 2,2,6,6-tetramethylpiperidine-1-oxyl (TEMPO), *N*-*tert*-butyl-2-methyl-1-phenylpropyl nitroxide (TIPNO), or *N*-*tert*-butyl-*N*-(1-diethylphosphono-2,2-dimethylpropyl) nitroxide (SG1, **1** in Scheme 1) are commercial or easy to synthesize.[1c,5] Several styrenic, (meth)acrylic and acrylamide monomers have already been polymerized in a controlled fashion by NMP.[1c,6] The latter class is however less studied in spite of the specific potential properties of their polymers such as temperature-dependent water solubility or high resistance to hydrolysis. The teams of Fischer, Gnanou, Hawker, and Schubert independently published successful results on the NMP of *N*,*N*-dimethylacrylamide

(DMAAm) in DMF in presence of either SG1[7] or TIPNO.[8] The effective NMP of *N*-isopropylacrylamide (NiPAAm) was described by both Harth *et al.* employing TIPNO[8] and Studer and co-workers using a highly sterically hindered TEMPO analogue.[9] O'Connor *et al.* also studied the polymerization of NiPAAm but using an interesting inverse suspension polymerization process in (supercritical carbon dioxide) $scCO_2$ in the presence of SG1.[10] Finally, we recently reported the synthesis of well-defined poly(*N*,*N*-diethylacrylamide) (PDEAAm) using the SG1-based ARKEMA BlocBuilder® technology (Scheme 1, **3**).[11]

In addition to its ability to control the radical polymerization of a wide range of monomers, NMP exhibits an interesting tolerance to water. For instance, Marx and co-workers managed to control the polymerization of styrene sulfonate (SSNa) in pure water thanks to a water-soluble TIPNO analogue.[12] Grassl *et al.* reported a reasonable control over the polymerization of acrylamide in homogeneous aqueous medium using a bicomponent system Vazo56/SG1[13] and Phan *et al.* published results on the control of DMAAm, SSNa, and 2-(acryloyloxy)ethylbenzyldimethylammonium chloride in aqueous solution using BlocBuilder®.[14] Chenal *et al.* reported the SG1-mediated polymerization of poly(ethylene glycol) methyl ether methacrylate (with a low amount of acrylonitrile) in hydroalcoholic solutions.[15] Recently Brusseau *et al.* successfully employed BlocBuilder® to control the polymerization of methacrylic acid in the presence of a low amount of SSNa in water.[16] Moreover, excellent results in terms of molar mass as well as particle size control were obtained with the use of water-soluble (macro)alkoxyamines (Scheme 1, **4**)[17] in aqueous dispersed media such as miniemulsion,[18] multi-step[19] and batch *ab initio*[16,20] emulsion.

Scheme 1. Structures of the nitroxide SG1 (1), the organosoluble SG1-based alkoxyamine MONAMS (2), the SG1-based alkoxyamine (BlocBuilder®, 3), and the SG1-terminated poly(acrylic acid) (PAA-SG1, 4).

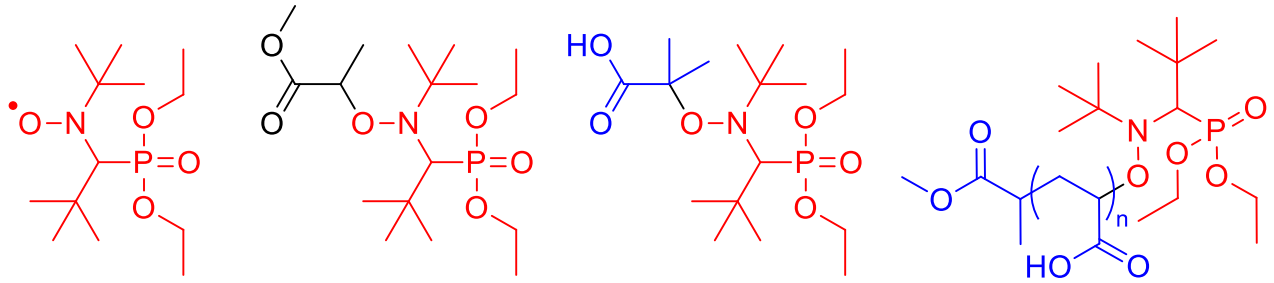

Poly(*N*,*N*-diethylacrylamide) (PDEAAm) is a thermoresponsive polymer. It exhibits a lower critical solution temperature (LCST)[21] around 32-33 °C like poly(*N*-isopropylacrylamide) (PNiPAAm).[22] DEAAm has the advantage of being a liquid which can make it easier to handle than NiPAAm and the volume phase transition of PDEAAm is more progressive than that of PNiPAAm.[23] DEAAm has already been employed to prepare hydrogels[24] and nano- and microgels.[25]

In this work we use SG1-capped poly(sodium acrylate) **4** to initiate the polymerization of DEAAm in water. This water-soluble macroalkoxyamine is able not only to initiate and mediate the polymerization but also to stabilize the particles formed by phase separation during the reaction. This *polymerization-induced self-assembly* process has recently received particular interest from different groups and is an important input in the difficult field of controlled radical polymerization in dispersed media.[26] Following the inspiring work of Ferguson *et al.* who have used a multi-step process to synthesize PAA-*b*-PS nanoparticles in water,[27] we used NMP to obtain stable latexes of permanently hydrophobic polymers with high solids content without the need for added surfactant or a sequential process.[20b,20c] We also reported the straightforward synthesis of thermoresponsive nanogels and pH-sensitive vesicles employing this approach.[25c,28] Other examples of this kind can be found using RAFT polymerization in water[25d,28b,29] but also in an organic medium.[30] Hereby we propose to use this approach to synthesize dynamic nanoparticles in a simple way. It will also be shown that special architectures are reachable with this technique, leading to physically core-crosslinked nanogels by controlled insertion of styrene units in the core. In addition to the dispersion polymerization kinetics, attention will be paid to the colloidal features of the nanoparticles as a function of pH, temperature, and salt concentration by dynamic light scattering (DLS), transmission electronic microscopy (TEM), and high-sensitivity scanning differential calorimetry (HSDSC).

Scheme 2. Nitroxide-mediated dispersion polymerization of DEAAm initiated by PAA-SG1 in basic water as conducted in this study.

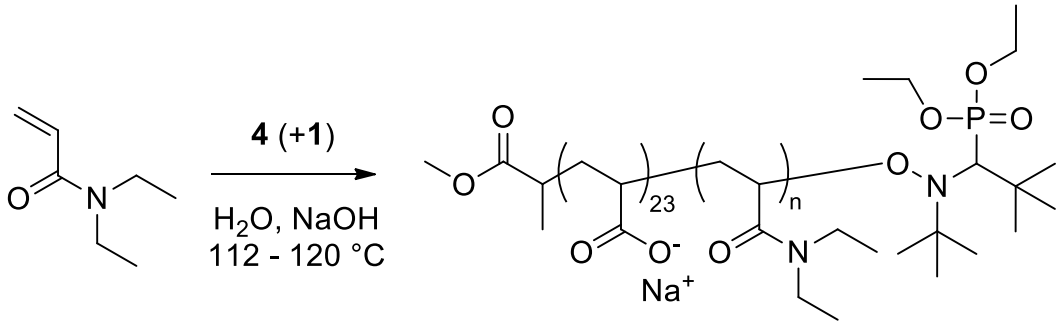

Experimental Part

Materials

Acrylic acid (AA, glacial), the alkoxyamine MONAMS **2**, and the nitroxide *N*-*tert*-butyl-*N*-(1-diethylphosphono-2,2-dimethylpropyl) (SG1, **1**, 88.5 %) were provided by Arkema and used as received. *N*,*N*-diethylacrylamide (DEAAm) was synthesized following a reported procedure.[31] Styrene was purchased from Acros and distilled under reduced pressure prior to use. Na_2CO_3 (Prolabo, pure), lithium bromide (LiBr, Rectapur, Prolabo), and *N*,*N*-dimethylformamide (DMF, Normapur, Prolabo) were used as received. NaOH solution was prepared by solubilization of 41 g of sodium hydroxide pellets (pure, SDS) into 1 L of deionized water.

*Synthesis of the SG1-capped poly(acrylic acid) macroinitiators **4***

Synthesis and characterization of the SG1-capped poly(acrylic acid) macroinitiators (PAA-SG1) were carried out following reported procedures.[6a,20b,32] Accordingly, the polymerization conditions were chosen to obtain the highest chain-end functionality. Therefore, high alkoxyamine initiator concentration and low polymerization time (low conversion) were selected to limit the occurrence of chain transfer to the solvent. The macroinitiators were purified by precipitation in diethyl ether and dried under vacuum at room temperature for 3 days. Two different samples with similar characteristics were used: M_n = 2000 g mol^{-1} (DP_n = 23, PDI = 1.15) for all experiments, except exps. 6 and 10 (Table 1), for which M_n = 2100 g mol^{-1} (DP_n = 24, PDI = 1.19). Chain-end functionality was above 90 mol% as determined by ^{31}P NMR using diethylphosphite as an internal standard.[32]

Dispersion polymerization of N,N-diethylacrylamide

The reactions were all carried out in batch, at 120 °C, under a 3-bar pressure of nitrogen, in a 300-mL thermostated glass reactor stirred at 300 rpm. In a typical recipe (experiment 4 in Table 1), DEAAm (30.03 g, 0.236 mol, 20.0 wt% based on water) and SG1 (29 mg, 84 μmol, 9.8 mol% based on PAA-SG1) were added at room temperature to a sodium hydroxide aqueous solution (120 mL, 1 equiv. NaOH based on the carboxylic acid groups and 37 mmol L_{aq}^{-1} of Na_2CO_3) of the required amount (1.73 g, 0.86 mmol, 7.31 mmol L_{aq}^{-1}) of the SG1-capped poly(acrylic acid) macroinitiator. The obtained homogeneous mixture was introduced into the preheated and stirred reactor, after nitrogen bubbling for 20 min at room temperature. The polymerizations were allowed to proceed for

24 hours in most cases to reach maximal conversion. During the polymerization course, 6-mL samples were withdrawn at regular time intervals to follow monomer conversion by gravimetry and analyze the polymer and the particles by methods described below. The various experimental conditions are reported in Table 1.

Semi-batch dispersion copolymerization of N,N-diethylacrylamide with styrene

Experiment 10 consists in a two-step process in which the first step is the same as described above for the homopolymerization of *N,N*-diethylacrylamide. 6-mL samples were withdrawn at regular time intervals to follow monomer conversion by gravimetry. Immediately after sample withdrawal at 5.5 h, 10.8 g of degassed styrene were injected (increasing the solids content to 26.9 wt% – after medium composition correction due to successive sample withdrawals) through a cartridge connected to the reactor via a valve allowing the process to occur under pressure and elevated temperature. Frequent sample withdrawal continued to proceed to follow the course of the reaction by gravimetry and size-exclusion chromatography.

Particle size analysis

The number-average or intensity-average particle diameters (D_n and D_i, respectively) and the dispersity factor (σ) were measured by dynamic light scattering (DLS) of diluted water suspensions at various temperatures and an angle of 90° with a Zetasizer Nano S90 from Malvern using a 4mW He-Ne laser at 633 nm. All calculations were performed using the Nano DTS software. For temperature cycles, values are reported at the equibrium of the system.

Size exclusion chromatography (SEC)

The polymers were separated by SEC in DMF (+ LiBr, 1 g L^{-1}, solvent filtered through 0.2-µm pore-size Millipore PTFE membranes) at 60 °C at a flow rate of 0.8 mL min^{-1}, with a polymer concentration around 5 mg mL^{-1} filtrated through a Whatman 0.45-µm pore-size PTFE membrane. Two Polymer Laboratories Mixed C columns (5 µm, 300 × 7.5 mm; separation limits: 200 – 1.9×10^6 g mol^{-1}) and a Polymer Laboratories Gel pre-column (50 × 7.5 mm) were used, while detection was performed with a differential refractive index (RI) detector (Viscotek, Dual 250). Eleven poly(methyl methacrylate) (PMMA) standards (Polymer Standards Service, molar mass at the peak from 200 to 1.9×10^6 g mol^{-1}) were used to calibrate the columns. The universal calibration curve was estimated from the PMMA calibration curve and the Mark-Houwink-Sakurada relation. The following Mark-Houwink-Sakurada relation was determined from the critical assessment of literature values (see Supporting Information):

$$[\eta] = 10.048 \times 10^{-5} M^{0.6961} \quad (\text{dL g}^{-1}) \qquad (1)$$

Polystyrene standards fail to provide a universal calibration curve, assumingly because of adsorption onto the stationary phase (see Supporting Information). This may be due to the presence of trace of water in the DMF eluent.[33] Hydrodynamic volume distributions were calculated as described previously[34] (see also Supporting Information). The software OriginLab Origin was used for data treatment as well as PeakFit for deconvolutions.

High-sensitivity scanning differential calorimetry (HSDSC)

The temperature-induced phase transition of the block copolymers was evidenced by following the heat exchange in diluted solutions of dialyzed copolymers between 1 and 80 °C using a Nano DSC III calorimeter from Calorimetry Sciences Corp. The system consists of two capillary cells, respectively reference and sample, of 0.33 mL under pressure (6 bars). All samples were degassed under reduced pressure before injection. In a preliminary step, a baseline scan was recorded with a sample identical to the reference and subtracted from the sample scan to avoid solvent-related artefacts. All measurements were performed at a scan rate of 1 °C min^{-1}. The sample thermal history was eliminated by a first scan to elevated temperature. Acquisition and treatment were carried out with the DSCRun and CpCalc softwares, respectively. After baseline subtraction, the maximum of the transition corresponding to the phase transition temperature (PTT) was determined by differentiation.[35]

Transmission electron microscopy (TEM)

The copolymer particles were observed on a 200 keV JEOL JEM 2010 UHR microscope equipped with an ORIUS high-resolution CCD camera (Gatan). The calibration was made from an orientated gold film presenting the lattice planes (200) and (220) each separated by a distance of 0.204 and 0.143 nm respectively. The acquisition was done with the Digital Micrograph software from Gatan. Samples were prepared by dilution in deionized water, deposited on a copper grid covered with a thin carbon film, and dried at a suitable temperature depending on the desired morphology.

Nuclear magnetic resonance spectroscopy (NMR)

The ^{31}P NMR spectrum of the precipitated PAA was recorded in water solution (external lock with D_2O) in a 10 mm diameter tube at room temperature. The apparatus is a Bruker Avance 300 operating at the frequency of 121.44 MHz. The spectrum was recorded using the following conditions allowing quantitative analysis: spectroscopic width 75 ppm, a flip angle of 10°, relaxation delay of 20 s, digital resolution of 0.27 Hz pt^{-1}, and suppression of the NOE. To allow quantitative analysis of the end group, the polymer was carefully weighed and a known amount of diethylphosphite was added as an internal reference. The chemical shift scale was calibrated on the basis of the added diethylphosphite at 7.1 ppm.

Molar compositions of the copolymers were determined by ^{1}H NMR spectroscopy (250 MHz) in $CDCl_3$ solution, at 25 °C, in 5 mm tubes, using an AC250 Bruker spectrometer. To determine the PAA-*b*-PDEAAm copolymer composition, integrals of the signals corresponding to backbone protons of the two blocks and methylenic protons of PDEAAm lateral groups were compared. For PAA-*b*-PDEAAm-*b*-P(DMAAm-*co*-S) copolymer composition, integrals of the signals corresponding to the aromatic protons of the styrene units and the methylenic protons of DEAAm units were compared. For triad investigation, the PAA-*b*-PDEAAm-*b*-P(DMAAm-*co*-S) copolymer was analyzed by ^{13}C NMR in $CDCl_3$ solution at room temperature using a Bruker DRX 500 spectrometer, operating at a frequency of 125.7 MHz. Spectra were recorded using the following conditions, allowing quantitative analysis: spectral width 240 ppm with 64 K data points, flip angle of 20°, relaxation delay of 20 s, and the decoupler power switched off during the relaxation (no NOE). A zero filling (128 K) was applied prior Fourier transform leading to a digital resolution of 18×10^{-4} ppm per point (0.23 Hz pt^{-1}). The chemical shift scale was calibrated on the basis of the solvent peak (77 ppm).

Results and discussion

Aqueous dispersion polymerization of N,N-diethylacrylamide initiated and mediated by PAA-SG1

N,N-Diethylacrylamide is highly soluble in water within the whole usual temperature range whereas, as mentioned above, its homopolymer possesses a temperature-dependent behavior with a LCST of *ca.* 32 C°.[22] As it is necessary to carry out nitroxide-mediated polymerization at temperatures higher than 80 °C to ensure effective dissociation of the alkoxyamines, the growing PDEAAm blocks are insoluble in these conditions and the process corresponds to dispersion polymerization.

As previously described for nitroxide-mediated polymerization of hydrophobic monomers in aqueous emulsion, the polymerization was first conducted at 120 °C under 3 bars.[20a-c] The polymerization was very fast, *i.e.*, 95 % of conversion reached after only *ca.* 2 h. (Figure 1). The conversion *vs.* time plot did not show any sigmoidal shape like it was the case for styrene or *n*-butyl acrylate (*n*BA) under emulsion polymerization conditions.[20a-c] At 112 °C the polymerization slowed down, which can be useful in the case of the addition of a second batch of monomer at a precise DEAAm conversion (*vide infra*).[25c] 95 % of conversion could still be obtained after only 4 hours leading to a stable latex-like dispersion. It has been previously shown in several studies that adding a small amount of free nitroxide to the initial mixture can induce a faster establishment of the persistent radical effect (PRE), thus leading to a slower polymerization and a theoretically better macromolecular control.[18,36] For this purpose, 5 and 10 mol% SG1 were introduced with respect to the macroalkoxyamine concentration. The polymerization rate was

clearly affected by the initial amount of free nitroxide. After 4 hours only 60 % and 50 %, respectively, of DEAAm had reacted, reaching almost complete conversion after 10 to 20 hours. The effect of the SG1 initial concentration is in agreement with its participation in the polymerization process, *i.e.*, with the existence of an activation-deactivation equilibrium which controls the polymerization kinetics.[36] Interestingly, ln(1/(1-conversion)) increased linearly versus time, indicating a first order kinetics with respect to monomer and a constant concentration of propagating radicals. Although this trend is expected in homogeneous NMP conditions, dispersion polymerization process is acknowledged to be more complex.[37] Indeed, in the latter situation under classical radical initiation, the polymerization normally takes place in both the monomer-swollen particles and the continuous phase, with different initiator and monomer concentrations in both phases. In an NMP system initiated by a macroalkoxyamine, it should however be different. Indeed, after complete nucleation, the radical produced at the chain-end by alkoxyamine dissociation are only located within the particles, which become then the sole polymerization loci. Since the local monomer concentration is expected to decrease continuously (in contrast to emulsion polymerization in which it remains constant over a broad conversion range, leading to a zeroth kinetic order with respect to monomer), a first order kinetics does not seem surprising. The linearity of the ln(1/(1-conversion)) *vs.* time plot is thus an indication of a constant radical concentration, in agreement with the NMP process with excess free nitroxide.

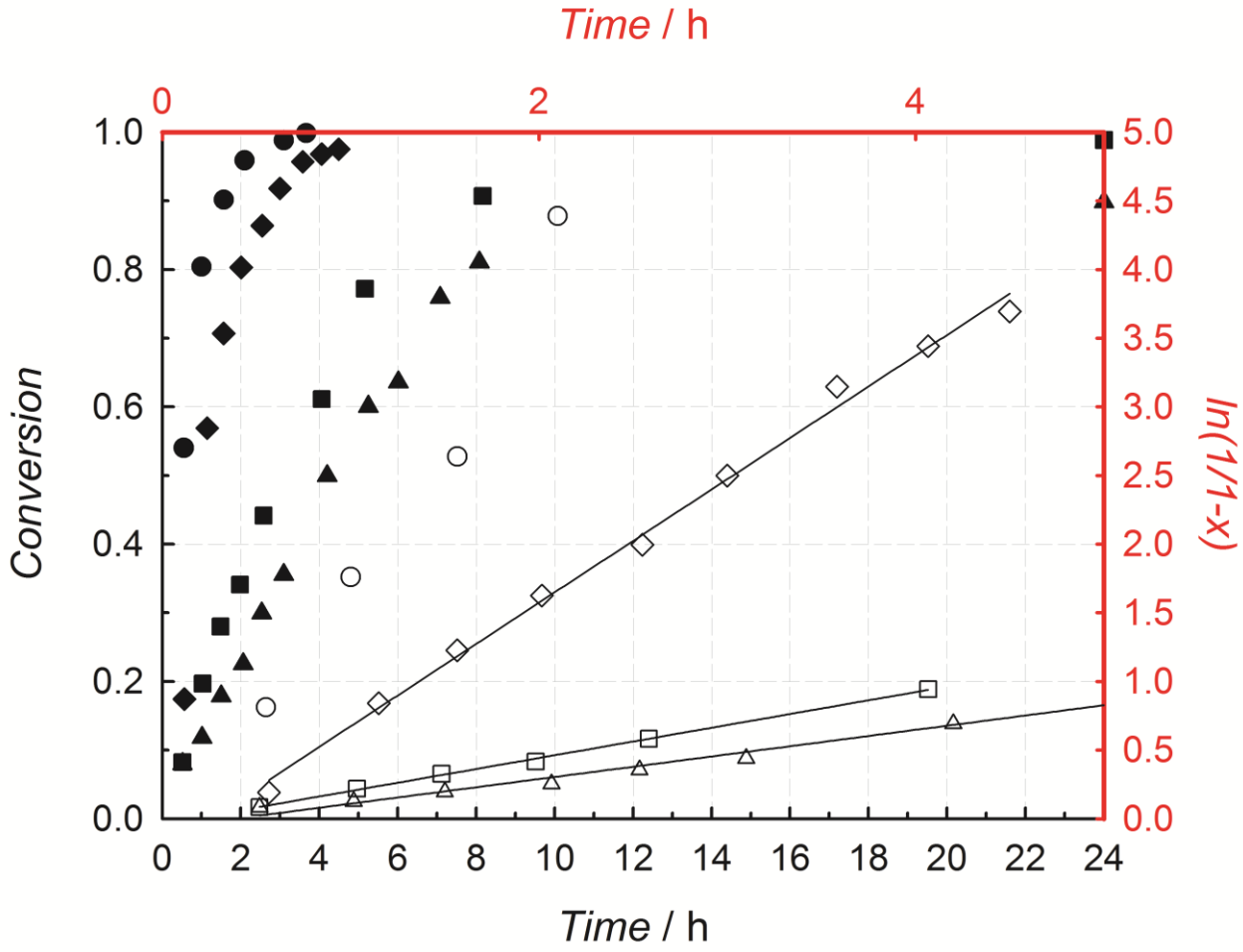

Figure 1. Conversion *vs.* time (full symbols) and first-order kinetic (empty symbols) plots for the dispersion polymerization of DEAAm (20 wt%) initiated by PAA_{23}-SG1 at different temperatures and different r = $[SG1]_0/[PAA\text{-}SG1]_0$ ratios [(Exp.1, ●) 120 °C, r = 0; (Exp. 2, ♦) 112 °C, r = 0; (Exp. 3, ■) 112 °C, r = 0.05; and (Exp. 4, ▲) 112 °C, r = 0.10]. Please note that the first-order kinetic plot is displayed only in its linear region and that no linear fit was applied to exp. 1 due to a rather limited number of data points.

We also investigated the influence of the alkoxyamine concentration on the polymerization. Figure 2 displays the evolution of monomer conversion with time for four different $[PAA\text{-}SG1]_0$. Although these experiments all resulted in very similar final results, a slight difference of behavior in the linear part of the first-order kinetic plot, *i.e.*, when the radical concentration is constant, was distinguishable. Indeed, the higher the alkoxyamine concentration, the slightly higher the ln(1/(1-conversion)) *vs.* time plot slope (*i.e.*, the higher the concentration of propagating radicals). This observation would be normally expected in the absence of initial free nitroxide. In the presence of an initial excess however, one may expect similar propagating radical concentration for an identical r = $[SG1]_0/[PAA\text{-}SG1]_0$ ratio (here r = 0.10).[38] This slight influence of the alkoxyamine concentration indicates that r = 0.10 is almost equal to (but

slightly below) the amount of free nitroxide needed to reach the activation-deactivation equilibrium (normally achieved by the persistent radical effect when r = 0).[34,36,37]

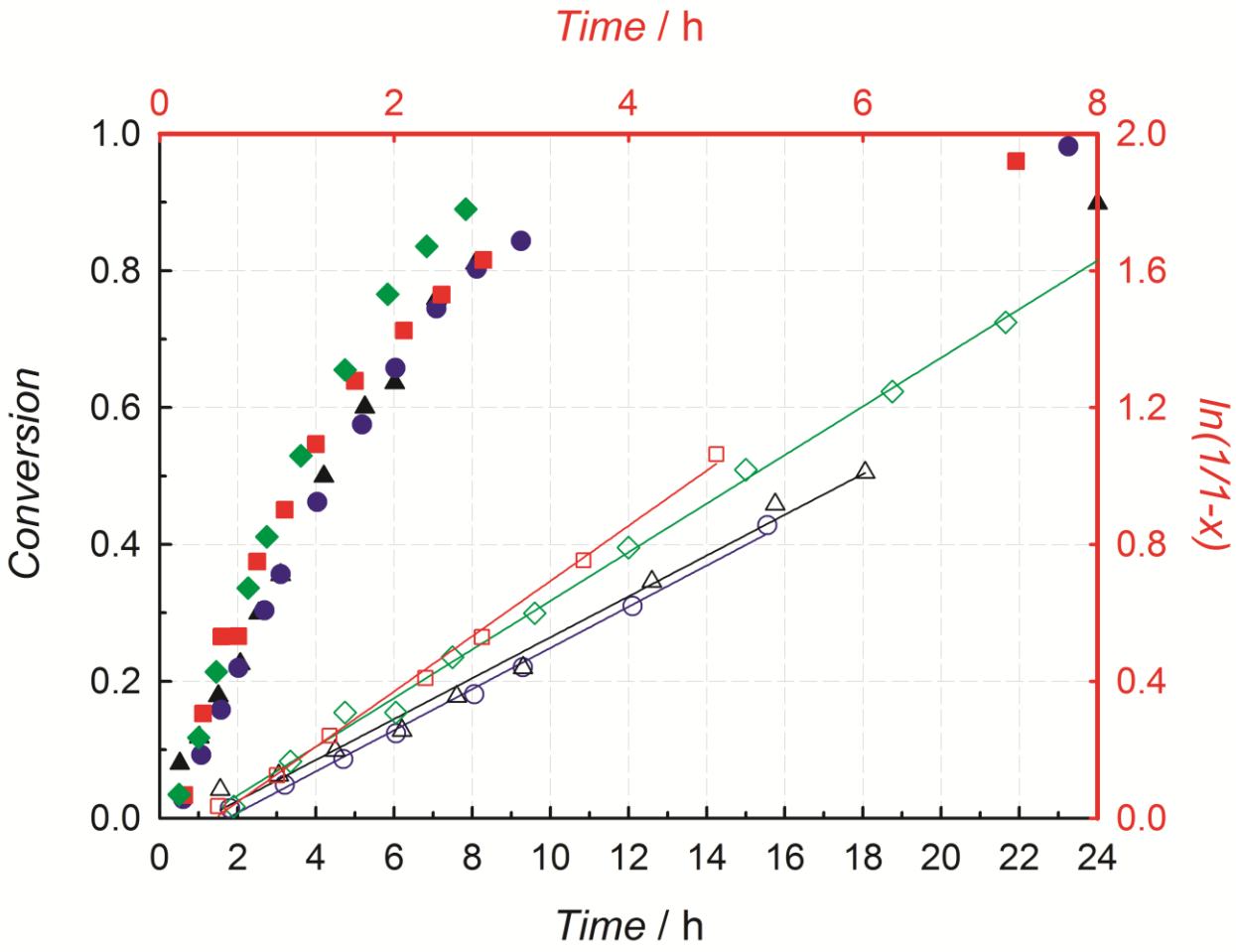

Figure 2. Conversion *vs.* time (full symbols) and first-order kinetic (empty symbols) plots for the dispersion polymerization of DEAAm (20 wt%) initiated by PAA_n-SG1 (n = 23–24) at r = $[SG1]_0/[PAA\text{-}SG1]_0$ = 0.10 and at different alkoxyamine concentrations [(Exp. 5, ●) $[PAA\text{-}SG1]_0 = 3.6 \times 10^{-3}$ mol L_{aq}^{-1}; (Exp. 4, ▲) $[PAA\text{-}SG1]_0 = 7.3 \times 10^{-3}$ mol L_{aq}^{-1}; (Exp. 6, ♦) $[PAA\text{-}SG1]_0 = 1.08 \times 10^{-2}$ mol L_{aq}^{-1}; and (Exp. 7, ■) $[PAA\text{-}SG1]_0 = 1.69 \times 10^{-2}$ mol L_{aq}^{-1}]. Please note that the first-order kinetic plot is displayed only in its linear region.

The first experiments were all based on a solids content of *ca.* 20 wt%. Although such a concentration is rather high for such a process as compared to the current literature, the results were satisfactory in terms of colloidal stability. Therefore, we carried out further experiments at even higher concentrations, *i.e.*, 29.3 and 39 wt%, while keeping a constant ratio of monomer to macroalkoxyamine. Figure 3 clearly evidences an alteration of the polymerization kinetics: the higher the solids content, the faster the polymerization. This may be related to a change in particle diameter, which decreased when the solids

content was increased (*i.e.*, concomitant increase in particle number – see Table 1). This would however seem to be in contradiction with the expected absence of compartmentalization effect in NMP in aqueous dispersed system,[20a,39] unless it corresponds to the increased polymerization rate predicted for very small particles.[39] It is noteworthy that, while at 20 wt% the medium remained fluid, at these higher concentrations it became quite viscous during the course of the reaction while maintaining a good colloidal stability.

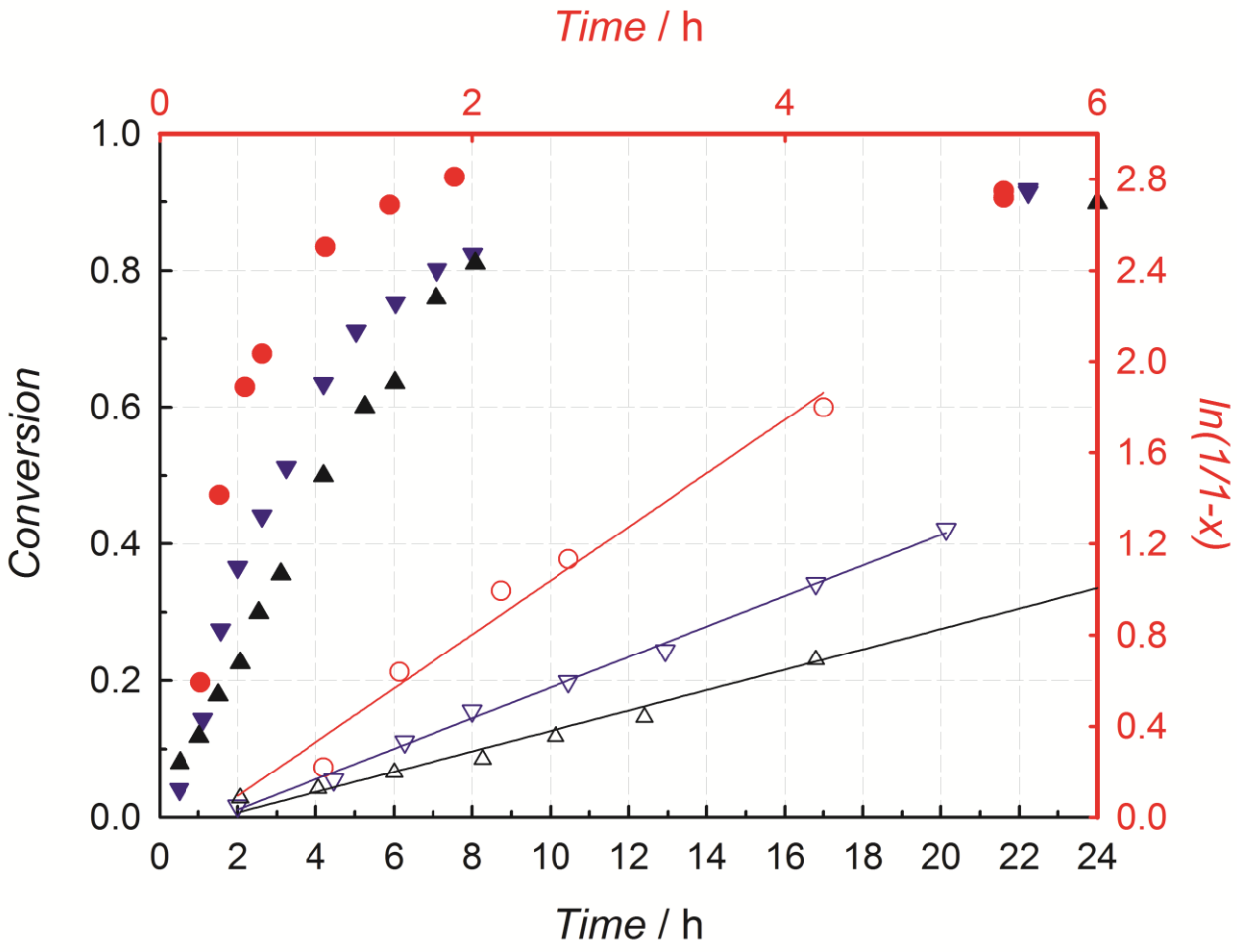

Figure 3. Conversion *vs.* time (full symbols) and first-order kinetic (empty symbols) plots for the dispersion polymerization of DEAAm initiated by PAA_{23}-SG1 at constant $[DEAAm]_0/[PAA\text{-}SG1]_0$ = 275 and r = $[SG1]_0/[PAA\text{-}SG1]_0$ = 0.10, and at different solids content [(Exp. 4, ▲) 19.9 wt%; (Exp. 8, ▼) 29.3 wt%; and (Exp. 9, ●) 39.0 wt%]. Please note that the first-order kinetic plot is displayed only in its linear region.

Size-exclusion chromatography analysis - hydrodynamic volume distributions

Since substituted polyacrylamides are prone to the formation of aggregates in classical SEC conditions in THF,[40] DMF/LiBr was chosen as the eluent. The chromatograms revealed bimodal distributions for

some of the samples (see Figure S4). The low hydrodynamic volume peak (a few tens of thousands g mol^{-1} in PMMA equivalent) was always observed and constantly shifting to higher hydrodynamic volumes during the course of the polymerization whereas the larger species peak (several hundreds of thousands g mol^{-1} in PMMA equivalent) was appearing randomly (Figure S6). The latter peak is thus assigned to aggregates.[41] Non-reversible intermolecular aggregation of homoPNiPAAm is attributed to hydrogen bonding when brought to complete dryness preventing it from full redissolution in a SEC eluent such as THF.[40] Block copolymers of PAA and PNiPAAm, a system very close to the present one, form hydrogen-bonded interpolymer complexes arising from interactions between acid and amide groups of the two respective blocks at room temperature.[42] Our SEC sample preparation includes drying and then acidifying the PAA block to ensure dissolution in DMF. This procedure probably favors the complexation of AA units with DEAAm ones. Addition of quaternary ammonium salts (benzyltrimethylammonium chloride or dibenzyldimethylammonium chloride) which would displace hydrogen bonds and render the PAA block organosoluble before SEC did not alter the aggregate peak. Assuming that water was responsible for the aggregation during the sample drying process,[40] the samples were dried after acidification by stirring in DMF on magnesium sulfate. Unfortunately, we did not observe any significant difference. We finally used a previously described methylation method to turn the carboxylic acid groups into methyl esters.[6a,32] This technique allowed the disruption of some aggregates but not in a quantitative way (Figure S5). Thus, the frequent overlapping of the two peaks of unimers and aggregates prevented us from determining any accurate average molar mass or hydrodynamic volume for the diblock copolymers.

In addition to this aggregation issue, the relatively different nature of the blocks can also pose a problem when converting raw elution data to molar mass values. Indeed the two components of the block copolymer have a molar mass distribution with no expected correlation between the PDI of both blocks. Some copolymer chains of the same hydrodynamic volume can have different molar masses due to differences in composition.[43] This may lead to a significant local dispersity,[44] *i.e.*, an incomplete SEC separation in terms of molar mass. Local dispersities significantly higher than unity have been measured for branched polymers,[45] leading to up to 100 % error on the determined molar masses.[46] In these cases, hydrodynamic volume distributions (HVD) are not affected by this error and have been proposed to replace molar mass distribution (or raw chromatograms).[47] HVDs are reproducible, contrary to raw chromatograms, which depend for example on the particular set of columns used. HV is a physical quantity characterizing the polymer (although molar mass is far more common), while elution time is only an experimental variable. HVDs have already been successfully used to study the synthesis of diblock copolymers.[34] Hydrodynamic volume distributions were thus used in this work instead of molar

mass distributions (for calculation of HVDs, refer to Supporting Information and previously published work[44c]).

Despite the aggregation phenomenon, most of the hydrodynamic volume distributions can be determined and compared – particularly their peak maxima – if the SEC data are deconvoluted. There is no recognized method to deconvolute SEC data. Deconvolution is usually not performed even on complex polymeric materials.[48] Gaussian functions have been used to deconvolute SEC peaks corresponding to star and linear polymers obtained by RAFT polymerization,[49] as well as multimodal molar mass distributions from SEC for star polymers produced by ATRP and *click* chemistry.[50] Barner-Kowollik however showed the limitation of this method.[51] The peak maxima of the convoluted and then deconvoluted molar mass distributions can indeed significantly differ. One explanation is that Gaussian functions do not properly fit SEC data because of the presence of band-broadening that require using exponentially modified Gaussian functions.[52] In the present work, we compared deconvolution based on Gaussian and on exponentially modified Gaussian functions. The exponentially modified Gaussians clearly gave lower residues and were thus chosen (see Supporting Information). The deconvolution was performed on the chromatograms (Figure S10) and the deconvoluted polymer peak was then converted into hydrodynamic volume distribution (Figure S12). Although it was impossible to obtain M_n = f(conversion) plots which are usually required to assess the controlled character of a polymerization, the overlay of the HVDs at different conversions were found to be rather conclusive. Indeed a constant shift towards higher hydrodynamic volumes was observed for all experiments (see Figures 4 and S13-S15). The traces were rather uniform, although a tailing phenomenon could be detected when monomer conversion increased, indicating a possibly slow and continuous initiation step due to rather unfavorable kinetic features between macroalkoxyamines bearing a terminal acrylic acid unit and macroalcoxyamines having already grown a second block. This phenomenon was for instance observed during the emulsion polymerization of *n*BA and styrene using the same initiating system.[20a-c] Thanks to the HVDs it was also possible to evaluate the influence on the macromolecular characteristics of diverse parameters discussed above in terms of kinetics. For instance, Figure 4 depicts the HVDs at different monomer conversions for experiments in which the macroalkoxyamine concentration was varied, all other parameters being identical. From top (Figure 4a) to bottom (Figure 4c), $[PAA\text{-}SG1]_0$ increases, so that the targeted molar mass at complete conversion decreases. For comparable monomer conversions (65–71 %, full line in red), when the macroalkoxyamine concentration increased, the hydrodynamic volume was clearly lower. Moreover, the HVDs became narrower with an increasing PAA-SG1 concentration. All these observations undoubtedly indicate that the polymerization proceeded in a controlled fashion.

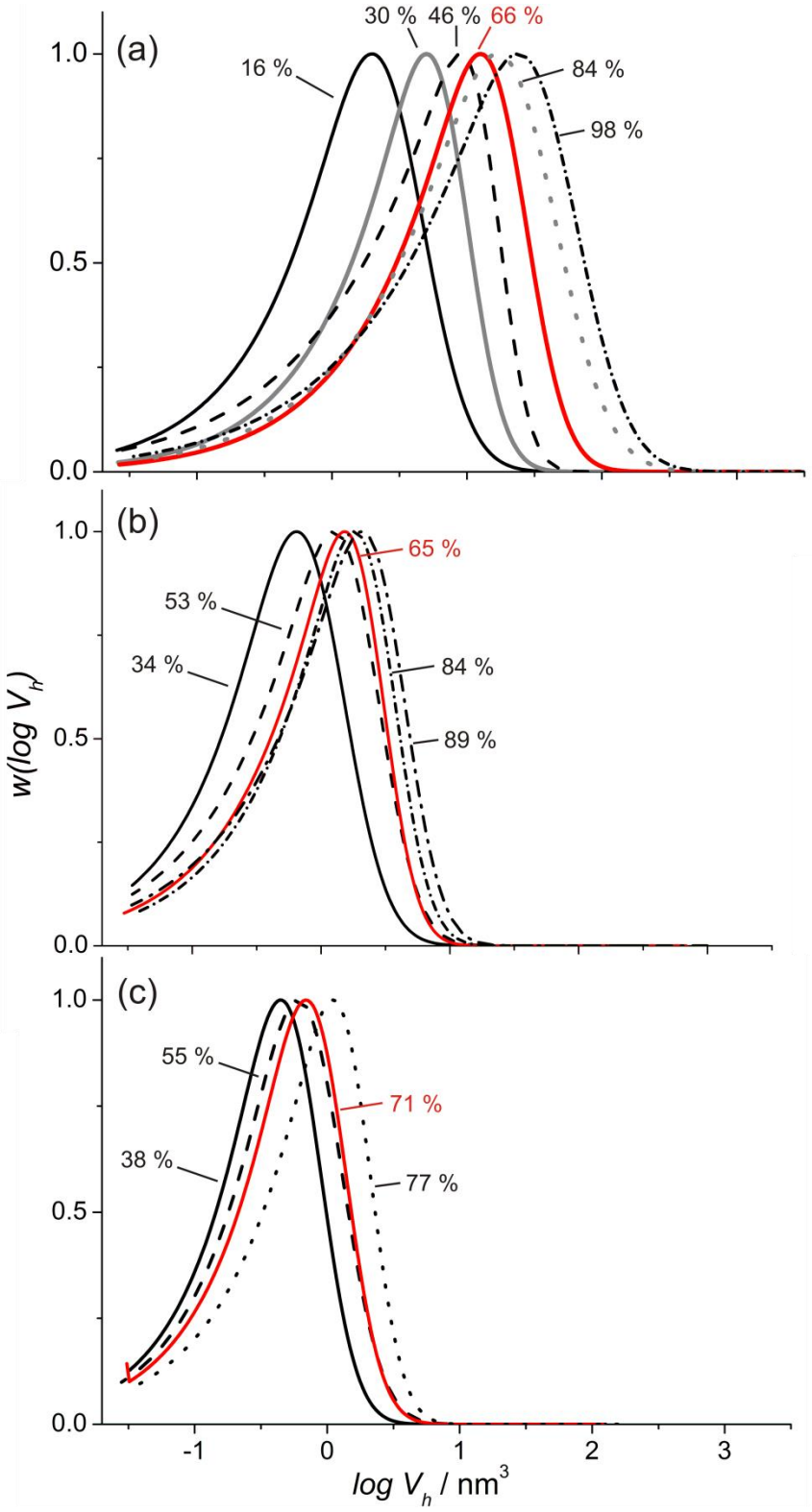

Figure 4. Overlay of hydrodynamic volume distributions at different monomer conversions for the dispersion polymerization of DEAAm (*ca.* 20 wt%) initiated by PAA_{23}-SG1 at different alkoxyamine concentrations [(a) Exp. 5, $[PAA\text{-}SG1]_0 = 3.6 \times 10^{-3}$ mol L_{aq}^{-1}; (b) Exp. 6, $[PAA\text{-}SG1]_0 = 1.08 \times 10^{-2}$ mol L_{aq}^{-1}; and (c) Exp. 7, $[PAA\text{-}SG1]_0 = 1.69 \times 10^{-2}$ mol L_{aq}^{-1}].

Colloidal characteristics and stimuli-sensitivity of the PAA-b-PDEAAm dispersions

Before the start of the reaction, the medium was transparent and colorless. It then progressively turned bluish to finally yield a white latex when maintained at high temperature. Upon cooling, a transparent and colorless solution was obtained again. For all experimental conditions, stable latexes (no coagulate) were recovered at the end of the reaction. Performing dynamic light scattering measurements at 50 °C on samples directly after withdrawal – not cooled below the phase transition temperature (PTT) – allowed us to determine the diameter of the particles formed during the dispersion polymerization process. A droplet was carefully taken off the sample with a preheated Pasteur pipette and then diluted in preheated deionized water. The nanoparticles formed during the process were in the 30–110 nm range with a rather narrow distribution (σ = 0.02–0.20), similarly to what was obtained in the case of styrene or *n*BA emulsion polymerization.[20a-c] The robustness of the system is emphasized once more by the fact that, for example, when the initial concentration of free nitroxide was varied with all other parameters remaining constant, the diameter of the final particles remained strictly the same (70 nm for exps. 2, 3, and 4). The average diameter of the particles could be lowered by increasing the amount of macroalkoxyamine which also plays the simultaneous role of stabilizer, while keeping the initial DEAAm concentration constant (*i.e.*, decreased theoretical degree of polymerization of the PDEAAm block) (Table 1, exps. 4-7). Nanoparticles with diameters as low as 30 nm could thus be produced. More generally, the particles were smaller when the degree of polymerization of the hydrophobic block was lower (see Figure S16).

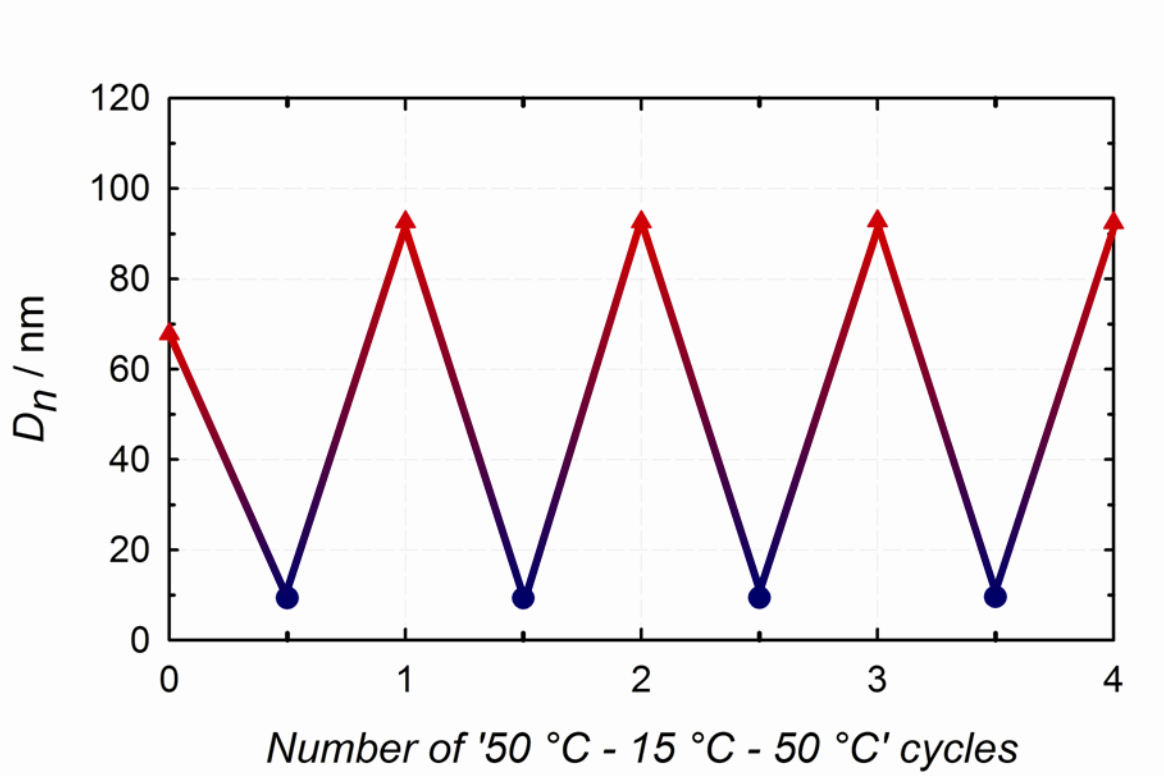

Figure 5. Evolution of the number-average hydrodynamic diameter (D_n) during cooling and heating cycles for the final PAA-*b*-PDEAAm copolymer from exp. 4 at pH = 11 [(▲) 50 °C and (●) 15 °C].

As previously mentioned, PDEAAm exhibits a LCST of 32–34 °C. Therefore, upon cooling to temperatures below the LCST, the former hydrophobic core of the particles was expected to swell with water and dissociate by release of free soluble copolymer chains. Figure 5 confirms this prediction in the case of exp. 4. Initially the particles had a diameter of 70 nm. After a first cooling at 15 °C, only free chains with a hydrodynamic diameter of about 10 nm were detected by DLS. When the newly formed homogeneous solution was heated again above the theoretical LCST, *e.g.*, at 50 °C in the present case, nanoparticles were reformed, however with a larger size than the initial ones (95 nm). Repeating this procedure several times, *i.e.*, cooling down to 15 °C and heating up to 50 °C, gave the same values. This cycling experiment shows that the particles initially formed were trapped in an out-of-equilibrium state, likely to be determined by the composition of the copolymers when they self-assembled during the polymerization. Once disassembled and re-formed, the self-organization of long PDEAAm follows a different mechanism leading to a different particle size.

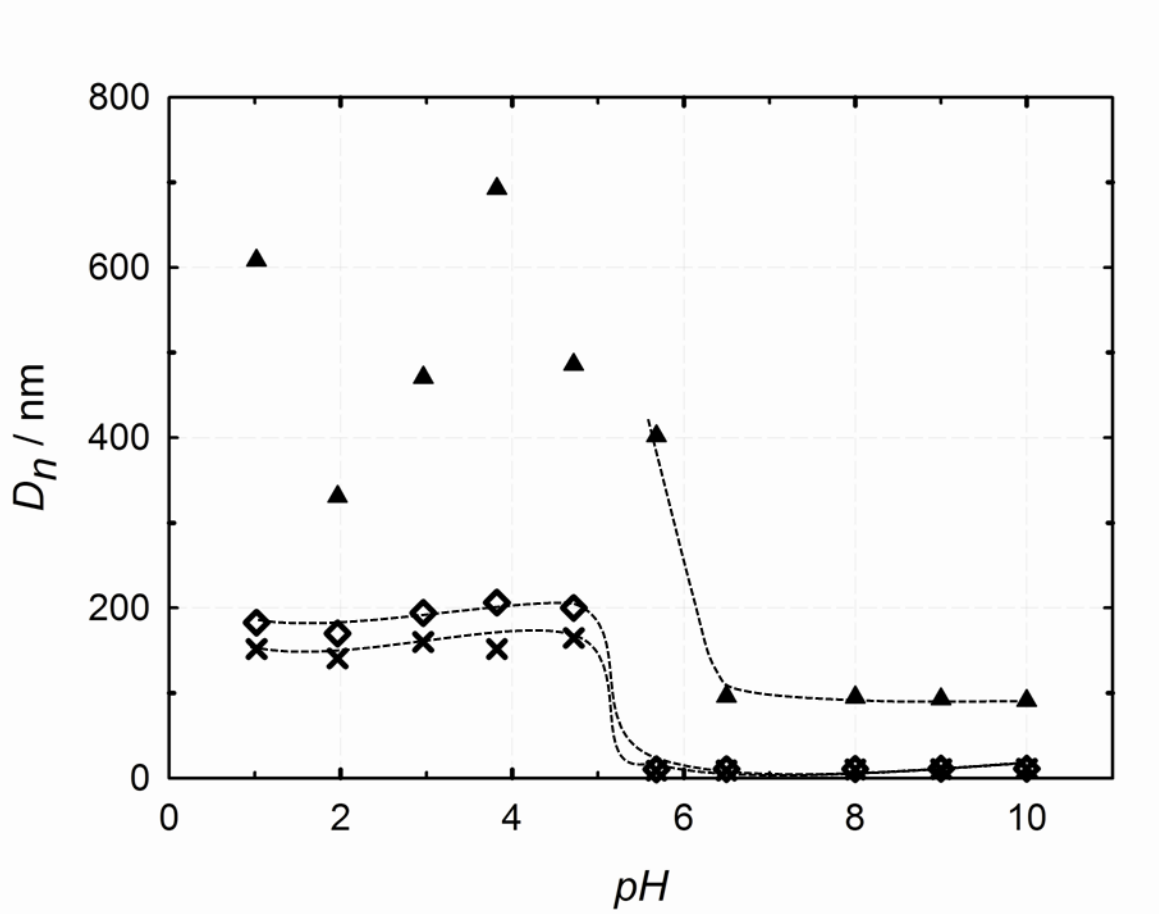

Figure 6. Evolution of the number-average hydrodynamic diameters with pH for the PAA-*b*-PDEAAm copolymers (exp. 4, final sample) at different temperatures [(**X**) 15 °C; (◊) 25 °C; and (▲) 50 °C]. Dotted lines are drawn to guide the eye.

Obviously, the PAA block imparts a pH-sensitive character to the copolymers and consequently to the particles in addition to the thermosensivity of the core. This type of double-responsive block copolymers has been previously coined as schizophrenic block copolymers.[53] Evidences for simultaneous pH- and temperature sensitive characters are displayed in Figure 6. At high pH values, the PAA block is in its ionized form (PANa) and is thus water-soluble. When the temperature is lower than the PTT of PDEAAm (15 °C or 25°C) – the thermosensitive block is thus also water-soluble – the measured diameters are very low, in the range of few nanometers and can be regarded as rough values for the free polymer chain dimensions in solution. At such low temperatures when the pH was decreased by adding aliquots of a 1 M hydrochloric acid aqueous solution, the diameters increased dramatically. Indeed the PANa block became re-protonated as the pKa is evaluated around 6.15[54] and the copolymers started to self-assemble into PAA-core particles. When the temperature was increased but remained below the PTT (25 °C), slightly larger assemblies were detected. When the temperature is higher than

the PTT at such acidic pH, both constitutive blocks are insoluble and the colloidal stability is largely affected, yielding undefined aggregates with large dimensions.

Scheme 3. Sketch of the proposed mechanism for PAA-SG1-initiated DEAAm dispersion polymerization and of the proposed solubilization-micellization behaviour of PAA-*b*-PDEAAm copolymers.

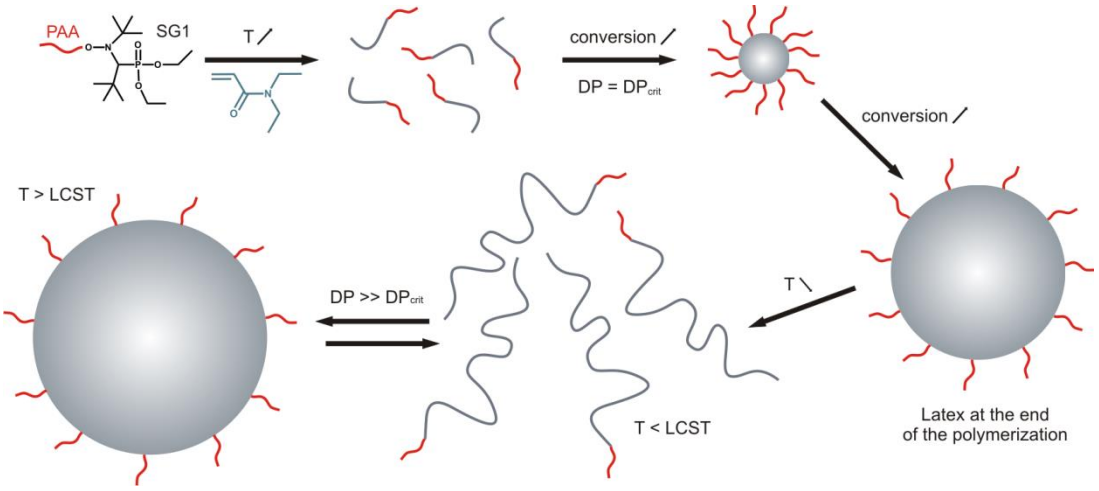

All the data collected and presented above led us to propose a possible scenario for the polymerization of DEAAm in water initiated by PAA-SG1 (Scheme 3). Initially the system is homogeneous and composed of an aqueous phase in which the macroinitiator and the monomer are dissolved. When the temperature is increased, alkoxyamine bonds start to reversibly disrupt and release PAA radicals and free nitroxides. Released radicals initiate the polymerization leading to the formation of a second block. When the PDEAAm block reaches a critical degree of polymerization (DP_{crit}), as the polymerization temperature is well above its PTT, it precipitates out of the aqueous phase to form PAA-stabilized micelles. Further propagation takes place in the organic phase to extend the hydrophobic block to its final degree of polymerization. At the end of the reaction, when the reactor is cooled down to room temperature, PDEAAm blocks become soluble and the aggregates start to swell and finally dissolve. As the temperature is increased again, PDEAAm becomes hydrophobic again and self-assembling takes place again. However, the dimensions of the re-formed particles are different (see Figure 5). As the system is composed of the exact same macromolecules as before the cooling disassembling process, it is clear that the block copolymer chains were initially trapped in out-of-equilibrium assemblies at the end of the polymerization. This can be explained by the nature of the assembling process: the first aggregation that takes place during the polymerization is governed by the length of the hydrophobic

block at low conversion: the short PDEEAm block drives the aggregation into star-like micelles during the nucleation period. As the polymerization proceeds in the so-formed nanoparticles the PDEEAm block grows and the final nanoparticles exhibit a much longer PDEEAm block. After a cooling-heating cycle, the diblock copolymer chains self-assemble into crew-cut micelles with a larger particle size [55]

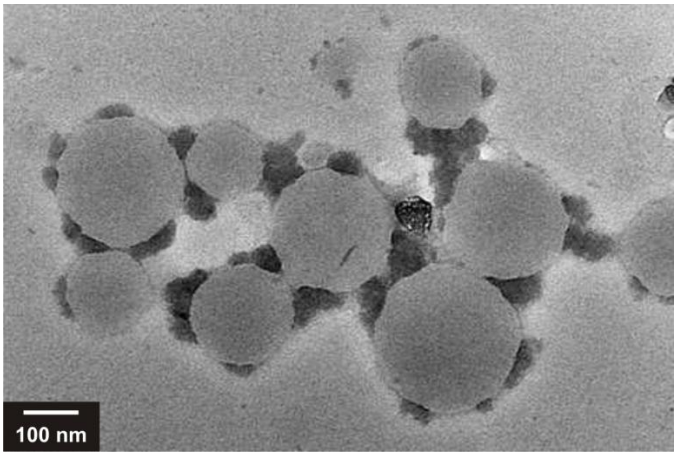

Figure 7. Electron micrograph of nanoparticles obtained by drying of a solution of PANa-*b*-PDEAAm at pH = 11 and at 80 °C.

The formation of nanoparticles from a block copolymer solution in good solvent conditions for PAA (pH = 11) was directly imaged by TEM. It should be noted that the visualization of the particles is not as easy as for tough PS particles for instance due to a lower electron absorbing nature and also the lower glass transition temperature of PDEAAm ($T_{g,PDEAAm}$ = 85 °C).[56] Figure 7 shows assemblies obtained by drying of a basic solution of PAA-*b*-PDEAAM at 80 °C, a temperature largely higher than the theoretical LCST. In agreement with the DLS data, spherical particles with diameters ranging from 90 to 150 nm and a rather large polydispersity can be observed. Note that the dry particles are surrounded by a shell of salts accumulating during the drying process (TEM imaging in dark-field mode showed diffraction).

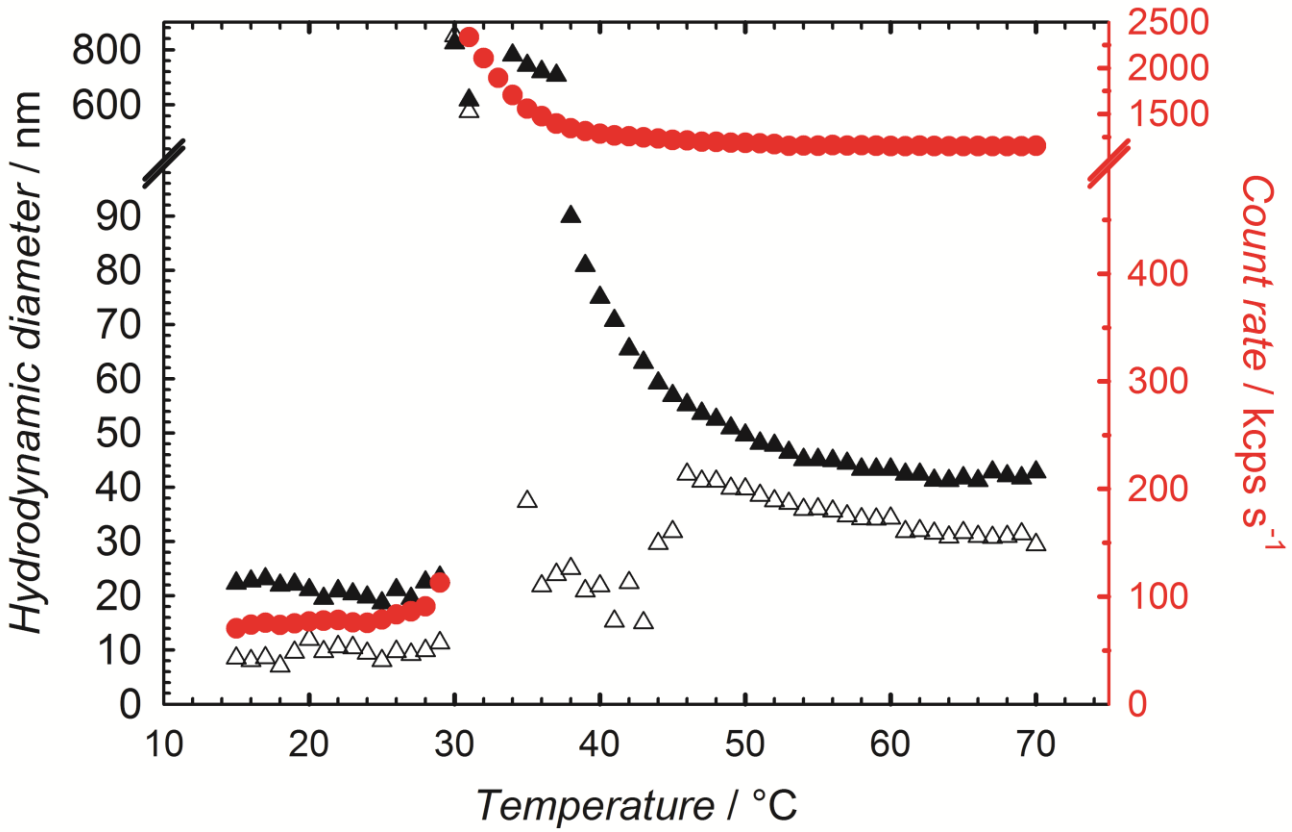

Figure 8. Evolution of the number-average (Δ) and intensity-average (▲) hydrodynamic diameters (D_n and D_i, respectively) and of the count rate (●) during the cooling of a PAA-*b*-PDEAAm copolymer solution at pH = 11 (Exp. 1).

We investigated further the particle dynamics with regards to their thermoresponsive behavior. For a sample at pH = 11, we followed by DLS the evolution of the hydrodynamic diameter during the cooling process. On Figure 8, the intensity- and number-average diameters as well as the count rate are plotted. Starting from 70 °C and cooling down to the PTT, we observed a slow and constant increase in both hydrodynamic diameters. However, the count rate remained rather steady until the temperature reached 38–36 °C when it increased suddenly. Around 32–30 °C, all the parameters plummeted dramatically to low values and remained almost constant over the 28–15 °C range. These measurements point at a slow swelling of the particles during the cooling process before a brutal disruption at the PTT. Furthermore when the critical temperature is approached, D_n values do not present any clear trend but rather fluctuate. It can be explained by the greater sensitivity of this value to the polydispersity of the sample compared to the intensity-average diameter which will hardly take into account small particles if large ones are present. We can thus assume that the swelling process originating from the PDEAAm block re-hydration is rather slow and that large aggregates are formed by swelling – hence D_i increase before

PTT – and progressively release free chains into the solution. Below the PTT, the measured diameters are low and can again be attributed to free chains in good solvent conditions. The count rate is particularly low confirming the absence of large scattering entities in the medium.

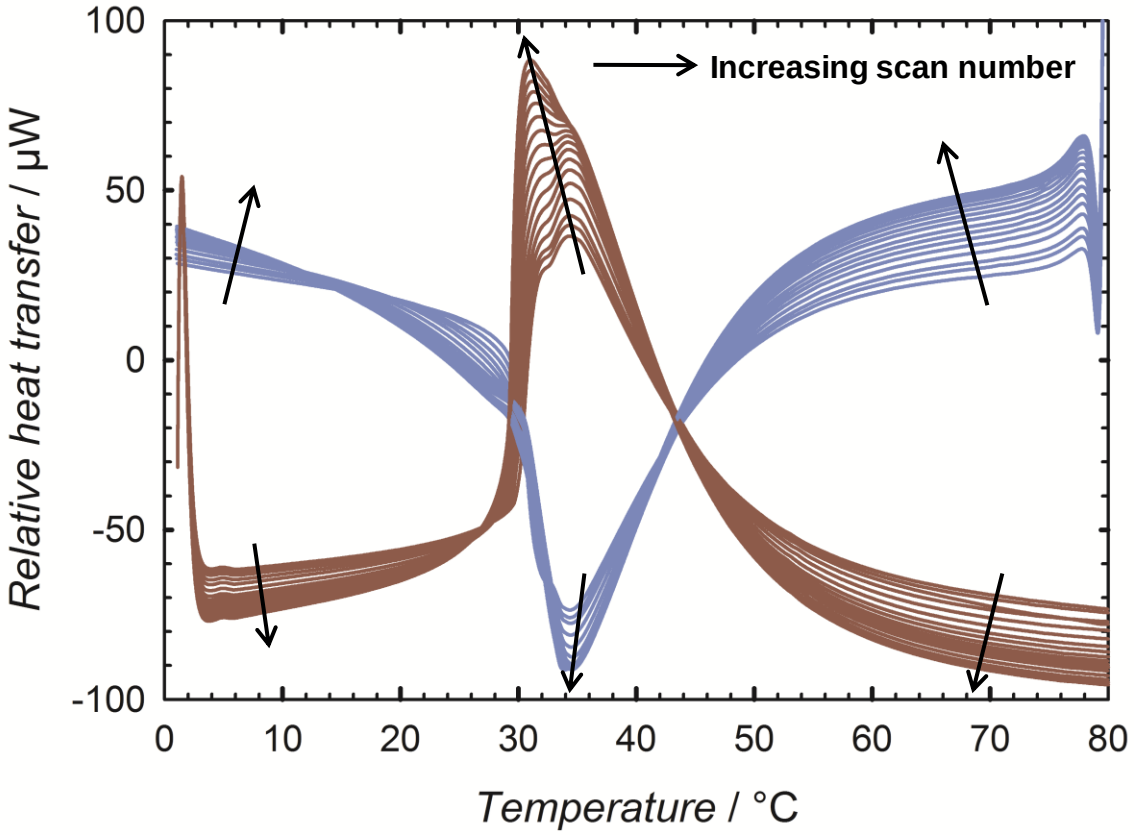

Figure 9. Heat transfer measured by HSDSC on a dialyzed solution of PAA-*b*-PDEAAm copolymers (Exp. 4, 5 g L^{-1}) at pH = 6.5. The dark-red curves represent the heating endothermic scans and the light-blue ones represent the cooling exothermic scans. Heating and cooling rates were 1 °C min^{-1}. The direction of the arrows indicates the increased number of scans.

High-sensitivity differential scanning calorimetry (HSDSC) gave us further insights into the temperature-induced phase transition. HSDSC is a technique able to measure very low heat exchanges. For instance, low-energy conformational changes of proteins such as unfolding or binding can be detected by this means.[57] This technique has already been used in the past to study thermosensitive polymer or microgel phase transition.[58] While DLS gives information at the nanometer-to-micrometer level, HSDSC enables us to reach the molecular level. It becomes then possible to detect the actual inset of the hydration or dehydration of the PDEAAm units, to know if the process is fully reversible, and also to determine an accurate phase transition temperature. Figure 9 confirms the existence of a PTT

situated around 32–34 °C, which is very close to the theoretical LCST.[22a] The transition is globally reversible since the heating and cooling curves are roughly inverted copies. It is also progressive as demonstrated by the width of the heat peaks: hydration and dehydration occur mostly between 25 and 60 °C, corroborating DLS data (see Figure 8). Two intensity maxima can be initially distinguished, particularly during the heating process. Snowden and Vincent observed the same phenomenon with P(NiPAAm-*co*-AA) microgels and attributed it to the presence of the carboxylate groups, with no further explanation.[58c] Figure 10 evidences the role of the acrylic acid units since an NMP-produced PDEAAm homopolymer[11] only showed one maximum using the exact same experimental method. By comparison, we could assign the lower-temperature maximum to the presence of the PAA block. On careful examination of Figure 9, we also noticed that the influence of the PAA segment was not so strong during the cooling process. It can be assumed that when the nanoparticles are already formed and the two blocks are segregated (above the PTT), the polyelectrolyte is less able to interact with the thermoresponsive block than when the chains are free in solution and at a higher entropy degree. Interestingly when the measurement was repeated several times, the peaks became narrower and, in the case of the heating ramp, the higher-temperature maximum tended to disappear which would signify a stronger effect of the supposed carboxylate group influence. The polymer chains possibly being at the end of the polymerization under high constraint (out-of-equilibrium state), we can suspect a progressive relaxation of the system. Furthermore if these HSDSC results and the DLS data are observed side-by-side (Figure 9 and 8, respectively) and the dissymmetry of the peaks is considered (at temperatures higher than the PTT, the area under the curve is significantly larger), it can be noted that the processes of dehydration or re-hydration in the micellar form are much slower than in the unimeric form.

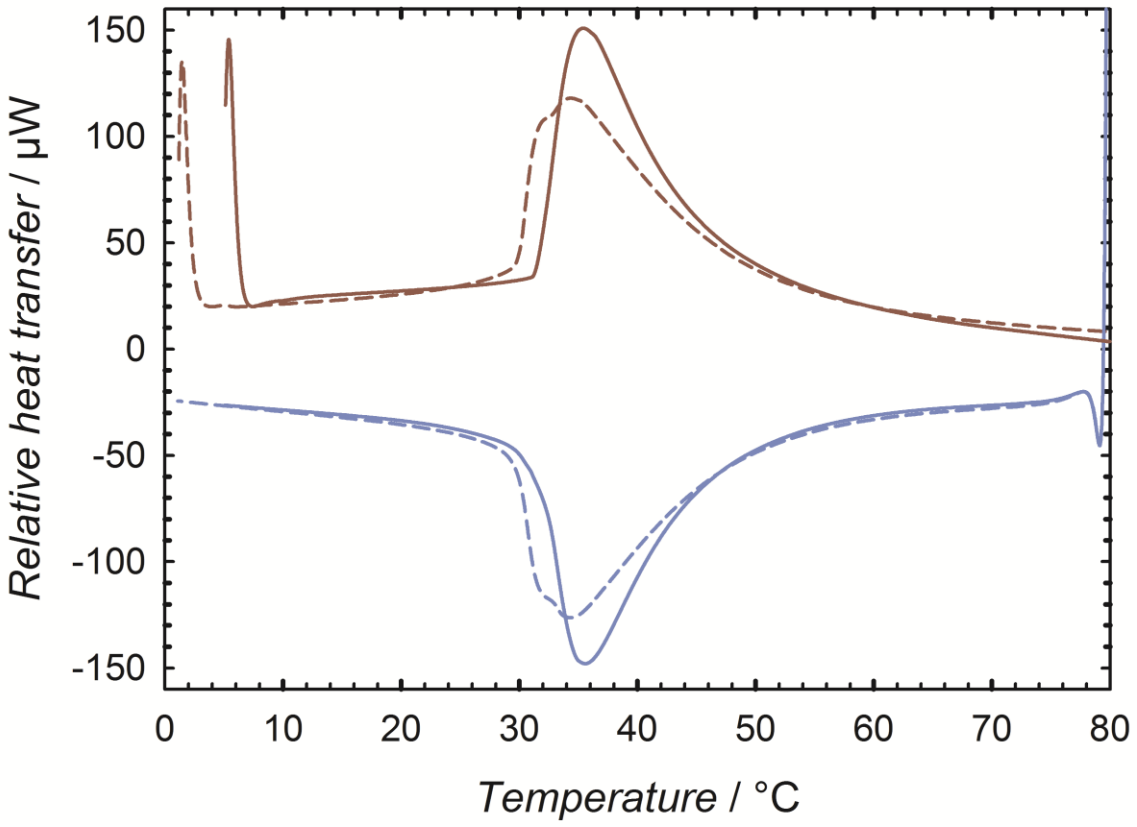

Figure 10. Heat transfer measured by HSDSC on a dialyzed solution of PAA-*b*-PDEAAm copolymers (dashed lines, Exp. 4, 5 g L^{-1}) and a solution of PDEAAm homopolymer (full lines, 5 g L^{-1}) at neutral pH. The dark-red curves represent the heating endothermic scans and the light-blue ones represent the cooling exothermic scans. Heating and cooling rates were 1 °C min^{-1}.

For potential uses of such nanogels, the influence of cosolutes is of major importance since very few applications actually take place in pure water. The effect of two different salts have been evaluated in this study, namely sodium chloride (NaCl) as a weak salting out agent and ammonium persulfate ($(NH_4)_2SO_4$), known as one of the strongest ones.[58a] In both cases, it was found that the PTT decreased progressively (almost linearly) with an increase in salt concentration (Figure 11). As expected, the influence of NaCl was less important than that of $(NH_4)_2SO_4$. At physiological ionic strength, *i.e.*, 0.2 M, the PTT was decreased to 30 °C in the case of NaCl but to almost 25 °C in the case of $(NH_4)_2SO_4$. In the thermograms (see Figure S17), only one temperature transition could be observed (one peak maximum) which seems to corroborate the aforementioned theory suggested by Snowden and Vincent.[58c] Indeed, the second peak which was attributed to the presence of the carboxylate groups was not present anymore, likely due to the increased ionic strength of the medium which screens charges.

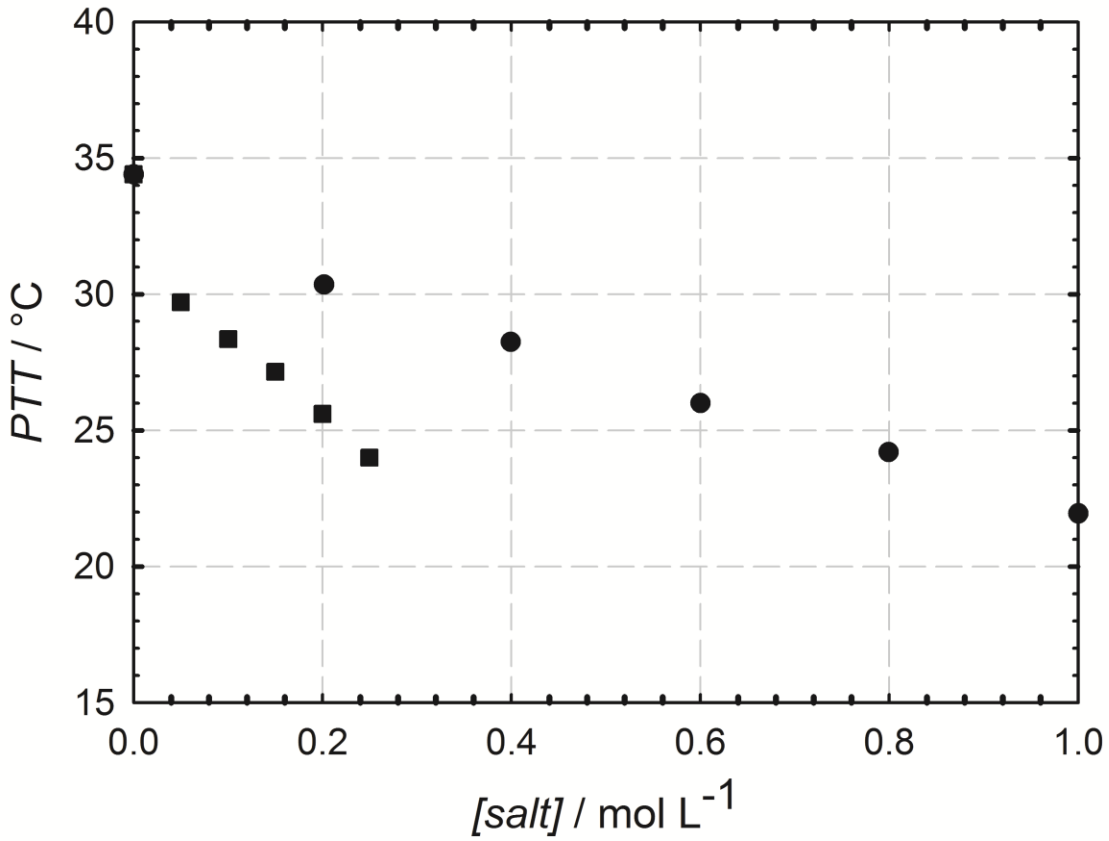

Figure 11. Evolution of the phase transition temperature (PTT) of PAA-*b*-PDEAAm copolymers (Exp. 4, 5 g L^{-1}) measured by HSDSC at neutral pH with a varying salt concentration for two different salts: sodium chloride (●) and ammonium persulfate (■).

Synthesis of core-shell-corona PS-PDEAAm-PAA physically crosslinked nanogels

Owing to the controlled/living nature of the nitroxide-mediated radical polymerization, it was possible to add a second batch of monomer meant to be inserted into the growing chains during the polymerization and create a third statistical block P(DEAAm-*co*-S). The idea was to use styrene to create a physical crosslinking by means of hydrophobic segregated nodules and thus freeze the *in situ* formed self-assembled structures and avoid their disassembly upon cooling.[59] For this purpose, after starting the polymerization with a procedure analogous to that of experiment 4, at 50 % of DEAAm conversion we added an amount of styrene such that the overall solids content reached 30 wt% (Exp. 10). As demonstrated by Figure 12, the polymerization continued to proceed but was slower – which is expected with styrene at this temperature – and reached a final overall conversion of about 70 % after 22 hours. At the end of the polymerization, a white latex was obtained. Contrary to the PAA-*b*-PDEAAm dispersions reported above, this latex remained stable upon cooling. The nanoparticle diameter D_n was 95 nm at 50 °C before cooling and 120 nm at 15 °C, proving the thermosensitivity of these physically

crosslinked nanoparticles exhibiting a PS core and a double hydrophilic block copolymer corona at room temperature.

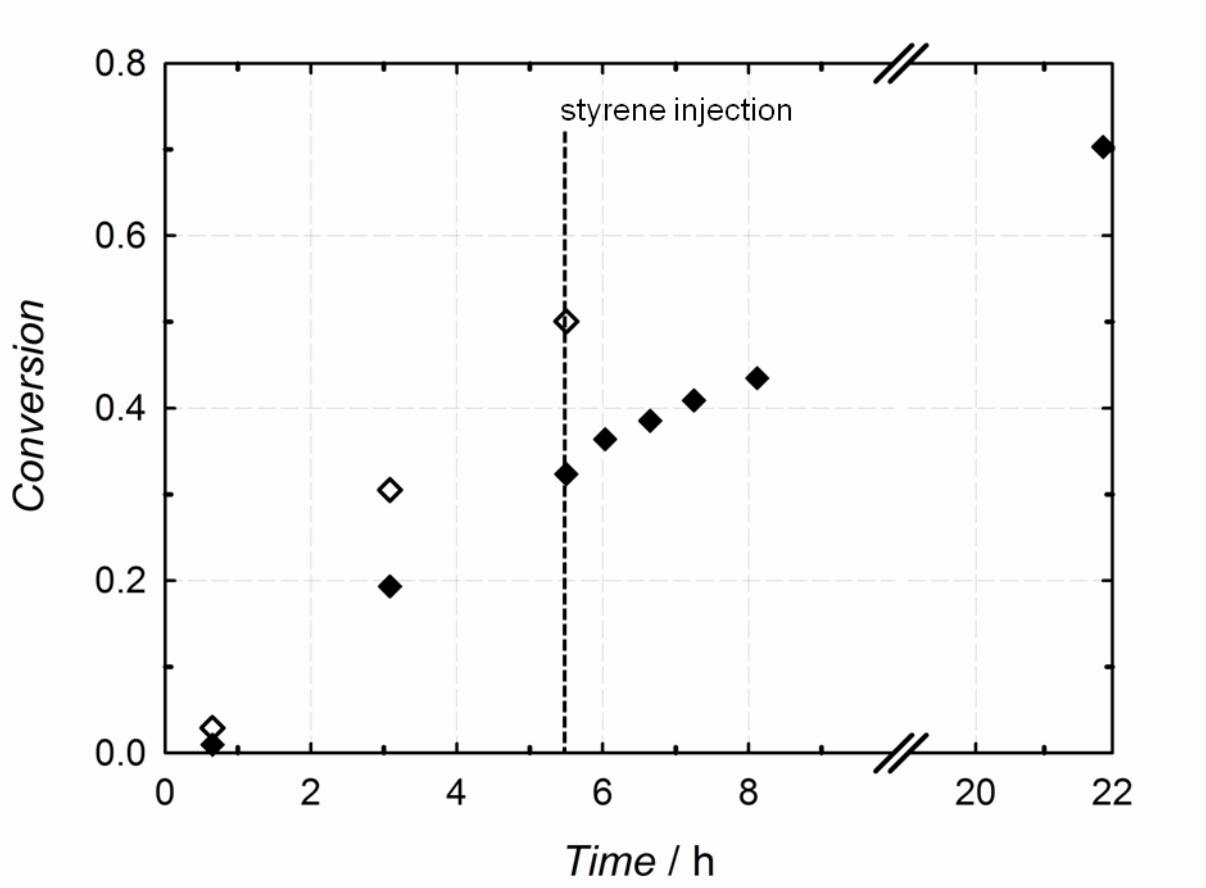

Figure 12. Monomer conversion versus polymerization time for the sequential dispersion-emulsion copolymerization of DEAAm and styrene initiated by PAA-SG1 at 112 °C (Exp. 10). Empty symbols: DEAAm conversion in the first step. Full symbols: Overall DEAAM/styrene weight conversion.

The same difficulties as previously reported in the current study with the PAA-*b*-PDEAAm system were encountered when we attempted the analysis of the styrene-containing copolymers by SEC. Nevertheless, we observed that HVD traces continuously shifted towards higher hydrodynamic volumes (Figure S15). In addition, we could try to calculate the copolymer composition employing diverse assumptions. By ^{1}H NMR, we calculated a DP_n close to 300 for the PDEAAm block at the injection of styrene. Assuming that the number of propagating chains remained constant throughout the polymerization and that the mass of monomer polymerized after the styrene addition was equally distributed among these chains, we calculated M_n = 34400 g mol^{-1} for the third block according to the conversion. Finally, by ^{1}H NMR performed on the dried triblock copolymer, we determined that the molar fractions of DEAAm and styrene units were equal to 0.71 and 0.25, respectively, in the entire copolymer. Considering that the copolymer exhibits a structure such as PAA_{24}-*b*-$PDEAAm_{300}$-*b*-$P(DEAAm_x$-*co*-$S_y)$ (Scheme 4), we determined x = 145 and y = 155.

Scheme 4. Assumed structure for the final triblock copolymer obtained by the sequential dispersion-emulsion copolymerization of DEAAm and styrene initiated by PAA-SG1 at 112 °C (Exp. 10).

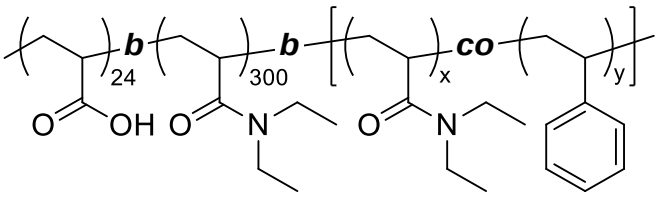

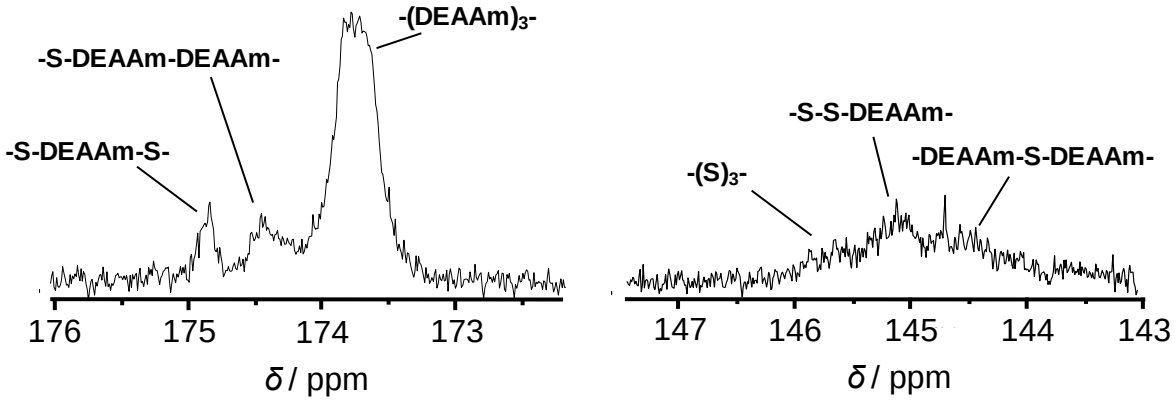

Figure 13. Selected regions (176–172 and 147–142 ppm) of the 300 MHz ^{13}C NMR spectrum in $CDCl_3$ of PAA-*b*-PDEAAm-*b*-P(DEAAm-*co*-S) block copolymer (Exp. 10).

^{13}C NMR allowed us to determine the microstructure of the triblock copolymers in analogy with results previously reported for a PS-P*n*BA system.[60] Indeed the triads centered on a styrene repeating unit (-$(S)_3$-, -$(S)_2$-DEAAm- et -DEAAm-S-DEAAm-) can be assigned thanks to the quaternary carbon having a chemical shift around 144.0–146.0 ppm. The triads centered on a DEAAm motif are identified by means of the carbonyl amide group carbon with a chemical shift at 173.5–175.0 ppm. According to Figure 13, the -$(DEAAm)_3$- triads form the largest population corroborating the presence of a long PDEAAm block (the center one). The main populations for triads centered on styrene seem to be -$(S)_2$-DEAAm- pointing at a third block rich in styrene with some DEAAm units, which would corroborate the inflection in polymerization rate. Previously determined reactivity ratios between styrene and DEAAm-related parent monomer DMAAm also points at a growing third block preferentially

incorporating styrene units at any monomer composition (see Figure S18).[61] Moreover, the relatively high hydrophobicity of styrene compared to DEAAm, which is strongly partitioned between the aqueous phase and the particles, certainly influences the process in that way. Unfortunately DSC measurements in the solid state (not shown) showed only a clear transition around 80 °C (close to the previously observed $T_{g,PDEAAm}$) and were thus not conclusive in this regard.

Conclusion

In the present report we have shown the synthesis of PAA-*b*-PDEAAm diblock copolymers by nitroxide-mediated aqueous dispersion polymerization employing a SG1-based poly(acrylic acid) macroalkoxyamine. This technique yielded double-responsive diblock copolymers and core-shell nanoparticles simultaneously. This presents some advantages over previous works using the more stringent anionic polymerization where a poly(acrylic acid) block had to be synthesized by hydrolysis of a poly(*t*-butyl acrylate) block and only after this step could the micellization in water take place.[31] We showed that out-of-equilibrium structures could be reached by such a process, which can present some interest when unconventional systems are desired. Our system is relatively versatile since it allows to work at high monomer content (20–40 wt%) and enables a delayed incorporation of hydrophobic (styrene) monomers to tune the responsivity or the structures of the aggregates. Thus core-shell-corona structures with a tough PS core were obtained in a one-pot procedure. Such architectures are usually not so straightforwardly obtained.[62] Temperature- and pH-responsive micelles have already found many applications in drug delivery which makes this system rather promising.[63]

Acknowledgements

G. D. thanks the French Ministry of Research for his PhD grant (2004-2007) and gratefully acknowledges financial support from the *Alexander von Humboldt Foundation* (Bonn, Germany) for his Humboldt Research Fellowship (2010-2012). The authors also thank for their help: C. Bui on monomer synthesis, S. Meghezi on the first explorations of the topic, O. Sepulchre (LCP) on SEC/DMF, Dr. Chris Garvey (ANSTO) and Dr. Glen Stone (UWS) for advice regarding deconvolution, V. Richard (former LRS) on TEM, Dr. M. Bellot (LCP) and Dr. L. Bouteiller (LCP) on HSDSC, and Arkema for providing SG1 and MONAMS as well as Prof. C. Chassenieux for fruitful discussions.

References

(1) (a) Solomon, D. H.; Rizzardo, E.; Cacioli, P. *Chem. Abstr.* **1985**, *102*, 221335q. (b) Solomon, D. H.; Rizzardo, E.; Cacioli, P. **1985**, EP135280. (c) Hawker, C. J.; Bosman, A. W.; Harth, E. *Chem. Rev.* **2001**, *101*, 3661-3688.

(2) (a) Braunecker, W. A.; Matyjaszewski, K. *Prog. Polym. Sci.* **2007**, *32*, 93-146. (b) Jenkins, A. D.; Jones, R. G.; Moad, G. *Pure Appl. Chem.* **2010**, *82*, 483- 491.

(3) (a) Matyjaszewski, K.; Xia, J. *Chem. Rev.* **2001**, *101*, 2921-2990. (b) Kamigaito, M.; Ando, T.; Sawamoto, M. *Chem. Rev.* **2001**, *101*, 3689-3745.

(4) (a) Moad, G.; Rizzardo, E.; Thang, S. H. *Aust. J. Chem.* **2005**, *58*, 379-410. (b) *Handbook of RAFT Polymerization*; Barner-Kowollik, C., Ed.; Wiley-VCH, Weinheim, Germany, 2008.

(5) (a) Matyjaszewski, K.; Woodworth, B. E.; Zhang, X.; Gaynor, S. G.; Metzner, Z. *Macromolecules* **1998**, *31*, 5955-5957. (b) Benoit, D.; Chaplinski, V.; Braslau, R.; Hawker, C. J. *J. Am. Chem. Soc.* **1999**, *121*, 3904-3920. (c) Wetter, C.; Jantos, K.; Woithe, K.; Studer, A. *Org. Lett.* **2003**, *5*, 2899-2902. (d) Chauvin, F.; Couturier, J.-L.; Dufils, P.-E.; Gerard, P.; Gigmes, D.; Guerret, O.; Guillaneuf, Y.; Marque, S. R. A.; Bertin, D.; Tordo, P. *ACS Symp. Ser.* **2006**, *944*, 326-341. (e) Nesvadba, P. *Chimia* **2006**, *60*, 832. (f) Braslau, R.; Tsimelzon, A.; Gewandter, J. *Org. Lett.* **2004**, *6*, 2233-2235. (g) Guillaneuf, Y.; Couturier, J.-L.; Gigmes, D.; Marque, S. R. A.; Tordo, P.; Bertin, D. *J. Org. Chem.* **2008**, *73*, 4728-4731. (h) http://www.arkema-inc.com/index.cfm?pag=860. (i) Harrisson, S.; Couvreur, P.; Nicolas, J. *Polym. Chem.* **2011**, *2*, 1859-1865.

(6) (a) Couvreur, L.; Lefay, C.; Belleney, J.; Charleux, B.; Guerret, O.; Magnet, S. *Macromolecules* **2003**, *36*, 8260-8267. (b) Bian, K.; Cunningham, M. F. *Macromolecules* **2005**, *38*, 695-701. (c) Bian, K.; Cunningham, M. F. *J. Polym. Sci., Part A: Polym. Chem.* **2006**, *44*, 414-426. (d) Lessard, B. t.; Marić, M. *Macromolecules* **2008**, *41*, 7870-7880. (e) Charleux, B.; Nicolas, J.; Guerret, O. *Macromolecules* **2005**, *38*, 5485-5492. (f) Dire, C.; Charleux, B.; Magnet, S.; Couvreur, L. *Macromolecules* **2007**, *40*, 1897-1903. (g) Nicolas, J.; Couvreur, P.; Charleux, B. *Macromolecules* **2008**, *41*, 3758-3761. (h) Ting, S. R. S.; Min, E. H.; Escalé, P.; Save, M.; Billon, L.; Stenzel, M. H. *Macromolecules* **2009**, *42*, 9422-9434. (i) Guillaneuf, Y.; Gigmes, D.; Marque, S. R. A.; Astolfi, P.; Greci, L.; Tordo, P.; Bertin, D. *Macromolecules* **2007**, *40*, 3108-3114. (j) Greene, A. C.; Grubbs, R. B. *Macromolecules* **2010**, *43*, 10320-10325. (k) Popescu, D.; Hoogenboom, R.; Keul, H.; Moeller, M. *Polym. Chem.* **2010**, *1*. (l) Hoogenboom, R.; Zorn, A.-M.; Keul, H.; Barner-Kowollik, C.; Moeller, M. *Polym. Chem.* **2012**, *3*.

(7) (a) Diaz, T.; Fischer, A.; Jonquieres, A.; Brembilla, A.; Lochon, P. *Macromolecules* **2003**, *36*, 2235-2241. (b) Schierholz, K.; Givehchi, M.; Fabre, P.; Nallet, F.; Papon, E.; Guerret, O.; Gnanou, Y. *Macromolecules* **2003**, *36*, 5995-5999. (c) Eggenhuisen, T. M.; Becer, C. R.; Fijten, M. W. M.; Eckardt, R.; Hoogenboom, R.; Schubert, U. S. *Macromolecules* **2008**, *41*, 5132-5140.

(8) Harth, E.; Bosman, A.; Benoit, D.; Helms, B.; Frechet, J. M. J.; Hawker, C. J. *Macromol. Symp.* **2001**, *174*, 85-92.

(9) Schulte, T.; Siegenthaler, K. O.; Luftmann, H.; Letzel, M.; Studer, A. *Macromolecules* **2005**, *38*, 6833-6840.

(10) O'Connor, P.; Zetterlund, P. B.; Aldabbagh, F. *J. Polym. Sci., Part A: Polym. Chem.* **2011**, *49*, 1719-1723.

(11) Delaittre, G.; Rieger, J.; Charleux, B. *Macromolecules* **2011**, *44*, 462-470.

(12) Nicolaÿ, R.; Marx, L.; Hemery, P.; Matyjaszewski, K. *Macromolecules* **2007**, *40*, 6067-6075.

(13) Grassl, B.; Clisson, G.; Khoukh, A.; Billon, L. *Eur. Polym. J.* **2008**, *44*, 50-58.

(14) Phan, T. N. T.; Bertin, D. *Macromolecules* **2008**, *41*, 1886-1895.

(15) Chenal, M.; Mura, S.; Marchal, C.; Gigmes, D.; Charleux, B.; Fattal, E.; Couvreur, P.; Nicolas, J. *Macromolecules* **2010**, *43*, 9291-9303.

(16) Brusseau, S.; D'Agosto, F.; Magnet, S.; Couvreur, L.; Chamignon, C.; Charleux, B. *Macromolecules* **2011**, *44*, 5590-5598.

(17) Charleux, B.; Nicolas, J. *Polymer* **2007**, *48*, 5813-5833.
(18) Nicolas, J.; Charleux, B.; Guerret, O.; Magnet, S. *Macromolecules* **2004**, *37*, 4453-4463.
(19) (a) Nicolas, J.; Charleux, B.; Guerret, O.; Magnet, S. *Angew. Chem. Int. Ed.* **2004**, *43*, 6186-6189. (b) Nicolas, J.; Charleux, B.; Guerret, O.; Magnet, S. *Macromolecules* **2005**, *38*, 9963-9973. (c) Nicolas, J.; Charleux, B.; Magnet, S. *J. Polym. Sci., Part A: Polym. Chem.* **2006**, *44*, 4142-4153.
(20) (a) Delaittre, G.; Charleux, B. *Macromolecules* **2008**, *41*, 2361-2367. (b) Delaittre, G.; Nicolas, J.; Lefay, C.; Save, M.; Charleux, B. *Chem. Commun.* **2005**, 614-616. (c) Delaittre, G.; Nicolas, J.; Lefay, C.; Save, M.; Charleux, B. *Soft Matter* **2006**, *2*, 223-231. (d) Dire, C.; Magnet, S.; Couvreur, L.; Charleux, B. *Macromolecules* **2008**, *42*, 95-103. (e) Brusseau, S.; Belleney, J.; Magnet, S.; Couvreur, L.; Charleux, B. *Polym. Chem.* **2010**, *1*, 720-729. (f) Groison, E.; Brusseau, S.; D'Agosto, F.; Magnet, S.; Inoubli, R.; Couvreur, L.; Charleux, B. *ACS Macro Lett.* **2011**, *1*, 47-51.
(21) (a) Heskins, M.; Guillet, J. E. *J. Macromol. Sci. Chem.* **1968**, *2*, 1441-1455. (b) Taylor, L. D.; Cerankowski, L. D. *J. Polym. Sci., Part A: Polym. Chem.* **1975**, *13*, 2551-2570.
(22) (a) Idziak, I.; Avoce, D.; Lessard, D.; Gravel, D.; Zhu, X. X. *Macromolecules* **1999**, *32*, 1260-1263. (b) Liu, H. Y.; Zhu, X. X. *Polymer* **1999**, *40*, 6985-6990.
(23) Tirumala, V. R.; Ilavsky, J.; Ilavsky, M. *J. Chem. Phys.* **2006**, *124*, 234911.
(24) Panayiotou, M.; Freitag, R. *Polymer* **2005**, *46*, 615-621.
(25) (a) Keerl, M.; Smirnovas, V.; Winter, R.; Richtering, W. *Macromolecules* **2008**, *41*, 6830-6836. (b) Saunders, J. M.; Alava, C.; Saunders, B. R. *Macromol. Symp.* **2007**, *251*, 63-71. (c) Delaittre, G.; Save, M.; Charleux, B. *Macromol. Rapid Commun.* **2007**, *28*, 1528-1533. (d) Rieger, J.; Grazon, C.; Charleux, B.; Alaimo, D.; Jérôme, C. *J. Polym. Sci., Part A: Polym. Chem.* **2009**, *47*, 2373-2390.
(26) (a) Oh, J. K. *J. Polym. Sci., Part A: Polym. Chem.* **2008**, *46*, 6983-7001. (b) Qiu, J.; Charleux, B.; Matyjaszewski, K. *Prog. Polym. Sci.* **2001**, *26*, 2083-2134. (c) Save, M.; Guillaneuf, Y.; Gilbert, R. G. *Aust. J. Chem.* **2006**, *59*, 693-711. (d) Zetterlund, P. B.; Kagawa, Y.; Okubo, M. *Chem. Rev.* **2008**, *108*, 3747-3794. (e) Cunningham, M. F. *Prog. Polym. Sci.* **2008**, *33*, 365-398.
(27) Ferguson, C. J.; Hughes, R. J.; Nguyen, D.; Pham, B. T. T.; Gilbert, R. G.; Serelis, A. K.; Such, C. H.; Hawkett, B. S. *Macromolecules* **2005**, *38*, 2191-2204.
(28) (a) Delaittre, G.; Dire, C.; Rieger, J.; Putaux, J.-L.; Charleux, B. *Chem. Commun.* **2009**, 2887-2889. (b) Zhang, W.; D'Agosto, F.; Boyron, O.; Rieger, J.; Charleux, B. *Macromolecules* **2011**, *44*, 7584-7593.
(29) (a) Bathfield, M.; D'Agosto, F.; Spitz, R.; Charreyre, M.-T.; Pichot, C.; Delair, T. *Macromol. Rapid Commun.* **2007**, *28*, 1540-1545. (b) dos Santos, A. M.; Le Bris, T.; Graillat, C.; D'Agosto, F.; Lansalot, M. *Macromolecules* **2009**, *42*, 946-956. (c) dos Santos, A. M.; Pohn, J.; Lansalot, M.; D'Agosto, F. *Macromol. Rapid Commun.* **2007**, *28*, 1325-1332. (d) Manguian, M.; Save, M.; Charleux, B. *Macromol. Rapid Commun.* **2006**, *27*, 399-404. (e) Shen, W.; Chang, Y.; Liu, G.; Wang, H.; Cao, A.; An, Z. *Macromolecules* **2011**, *44*, 2524-2530. (f) Grazon, C.; Rieger, J.; Sanson, N.; Charleux, B. *Soft Matter* **2011**, *7*, 3482-3490. (g) Chaduc, I.; Zhang, W.; Rieger, J.; Lansalot, M.; D'Agosto, F.; Charleux, B. *Macromol. Rapid Commun.* **2011**, *32*, 1270-1276. (h) Li, Y.; Armes, S. P. *Angew. Chem. Int. Ed.* **2010**, *49*, 4042-4046. (i) Sugihara, S.; Blanazs, A.; Armes, S. P.; Ryan, A. J.; Lewis, A. L. *J. Am. Chem. Soc.* **2011**, *133*, 15707-15713. (j) Semsarilar, M.; Ladmiral, V.; Blanazs, A.; Armes, S. P. *Langmuir* **2011**, *28*, 914-922.
(30) (a) Houillot, L.; Bui, C.; Save, M.; Charleux, B.; Farcet, C.; Moire, C.; Raust, J.-A.; Rodriguez, I. *Macromolecules* **2007**, *40*, 6500-6509. (b) Wan, W.-M.; Sun, X.-L.; Pan, C.-Y. *Macromolecules* **2009**, *42*, 4950-4952. (c) Houillot, L.; Bui, C.; Farcet, C. l.; Moire, C.; Raust, J.-A.; Pasch, H.; Save, M.; Charleux, B. *ACS Appl. Mater. Interfaces* **2010**, *2*, 434-442. (d) Huang, C.-Q.; Pan, C.-Y. *Polymer* **2010**, *51*, 5115-5121. (e) He, W.-D.; Sun, X.-L.; Wan, W.-M.; Pan, C.-Y. *Macromolecules* **2011**, *44*, 3358-3365.
(31) André, X.; Zhang, M.; Mueller, A. H. E. *Macromol. Rapid Commun.* **2005**, *26*, 558-563.

(32) Lefay, C.; Belleney, J.; Charleux, B.; Guerret, O.; Magnet, S. *Macromol. Rapid Commun.* **2004**, *25*, 1215-1220.
(33) Temyanko, E.; Russo, P. S.; Ricks, H. *Macromolecules* **2001**, *34*, 582-586.
(34) Hosseini Nejad, E.; Castignolles, P.; Gilbert, R. G.; Guillaneuf, Y. *J. Polym. Sci., Part A: Polym. Chem.* **2008**, *46*, 2277-2289.
(35) Throughout this study the terms LCST (lower critical transition temperature) and PTT (phase transition temperature) are independently employed. The LCST is the lowest PTT measured over the whole range of polymer concentration.
(36) Fukuda, T.; Goto, A.; Ohno, K. *Macromol. Rapid Commun.* **2000**, *21*, 151-165.
(37) Jiang, S.; Sudol, E. D.; Dimonie, V. L.; El-Aasser, M. S. *J. Polym. Sci., Part A: Polym. Chem.* **2008**, *46*, 3638-3647
(38) Goto, A.; Fukuda, T. *Prog. Polym. Sci.* **2004**, *29*, 329-385.
(39) Charleux, B. *Macromolecules* **2000**, *33*, 5358-5365.
(40) Ganachaud, F.; Monteiro, M. J.; Gilbert, R. G.; Dourges, M.-A.; Thang, S. H.; Rizzardo, E. *Macromolecules* **2000**, *33*, 6738-6745.
(41) It must also be noted that in some occurrences, within a same polymerization experiment, no high molar mass population was observed at all at intermediate monomer conversion while lower- or higher-conversion samples did show this population. This clearly evidences the fact that these populations are randomly formed after the polymerization and can be attributed to aggregation and not to potential branching or crosslinking of the chains during the polymerization process.
(42) Schilli, C. M.; Zhang, M.; Rizzardo, E.; Thang, S. H.; Chong, Y. K.; Edwards, K.; Karlsson, G.; Müller, A. H. E. *Macromolecules* **2004**, *37*, 7861-7866.
(43) (a) Gaborieau, M.; Castignolles, P. *Anal. Bioanal. Chem.* **2011**, *399*, 1413-1423. (b) Hamielec, A. E.; Ouano, A. C. *J. Liq. Chromatogr.* **1978**, *1*, 111-120.
(44) (a) Balke, S. T. In *Modern methods of Polymer Characterization*; 1st ed.; Barth, H. G., Mays, J. W., Eds.; John Wiley & Sons: New York, 1991; Vol. vol. 113; pp 1-66. (b) Balke, S. T.; Mourey, T. H. *J. Appl. Polym. Sci.* **2001**, *81*, 370-383. (c) Gaborieau, M.; Gilbert, R. G.; Gray-Weale, A.; Hernandez, J. M.; Castignolles, P. *Macromol. Theory Simul.* **2007**, *16*, 13-28. (d) Kostanski, L. K.; Keller, D. M.; Hamielec, A. E. *J. Biochem. Biophys. Methods* **2004**, *58*, 159-186. (e) Mourey, T. H.; Balke, S. T. *J. Appl. Polym. Sci.* **1998**, *70*, 831-835. (f) Mourey, T. H.; Vu, K. A.; Balke, S. T. *ACS Symp. Ser.* **1999**, *731*, 20-34.
(45) (a) Castignolles, P.; Graf, R.; Parkinson, M.; Wilhelm, M.; Gaborieau, M. *Polymer* **2009**, *50*, 2373-2383. (b) Gaborieau, M.; Nicolas, J.; Save, M.; Charleux, B.; Vairon, J.-P.; Gilbert, R. G.; Castignolles, P. *J. Chromatogr. A* **2008**, *1190*, 215-233.
(46) (a) Castignolles, P. *Macromol. Rapid Commun.* **2009**, *30*, 1995 - 2001. (b) Junkers, T.; Schneider-Baumann, M.; Koo, S. S. P.; Castignolles, P.; Barner-Kowollik, C. *Macromolecules* **2010**, *43*, 10427-10434.
(47) (a) Castignolles, P.; Gaborieau, M. *J. Sep. Sci.* **2010**, *33*, 3564–3570. (b) Hernández, J. M.; Gaborieau, M.; Castignolles, P.; Gidley, M. J.; Myers, A. M.; Gilbert, R. G. *Biomacromolecules* **2008**, *9*, 954-965.
(48) Netopilik, M.; Kratochvil, P. *Polym. Int.* **2009**, *58*, 198-201.
(49) (a) Boschmann, D.; Edam, R.; Schoenmakers, P. J.; Vana, P. *Polymer* **2008**, *49*, 5199-5208. (b) Boschmann, D.; Vana, P. *Macromolecules* **2007**, *40*, 2683-2693.
(50) (a) Gao, H. F.; Matyjaszewski, K. *Macromolecules* **2006**, *39*, 4960-4965. (b) Yang, H. J.; Jiang, B. B.; Huang, W. Y.; Zhang, D. L.; Kong, L. Z.; Chen, J. H.; Liu, C. L.; Gong, F. H.; Yu, Q.; Yang, Y. *Macromolecules* **2009**, *42*, 5976-5982. (c) Inglis, A. J.; Sinnwell, S.; Davis, T. P.; Barner-Kowollik, C.; Stenzel, M. H. *Macromolecules* **2008**, *41*, 4120-4126.
(51) Barner-Kowollik, C. *Macromol. Rapid Commun.* **2009**, *30*, 1625-1631.

(52) (a) Baumgarten, J. L.; Busnel, J. P.; Meira, G. R. *J. Liq. Chromatogr. Relat. Technol.* **2002**, *25*, 1967-2001. (b) Konkolewicz, D.; Taylor II, J. W.; Castignolles, P.; Gray-Weale, A.; Gilbert, R. G. *Macromolecules* **2007**, *40*, 3477-3487.
(53) Bütün, V.; Liu, S.; Weaver, J. V. M.; Bories-Azeau, X.; Cai, Y.; Armes, S. P. *React. Funct. Polym.* **2006**, *66*, 157-165.
(54) Burguière, C. Doctoral Thesis, Université Pierre et Marie Curie, Paris, **2001**.
(55) (a) Astafieva, I.; Zhong, X. F.; Eisenberg, A. *Macromolecules* **1993**, *26*, 7339-7352. (b) Zhang, L.; Eisenberg, A. *J. Am. Chem. Soc.* **1996**, *118*, 3168-3181.
(56) André, X. Doctoral Thesis, Universität Bayreuth, **2006**.
(57) (a) Freire, E. *Annu. Rev. Biophys. Biomol. Struct.* **1995**, *24*, 141-165. (b) Spink, C. H. *Methods Cell Biol.* **2008**, *84*, 115-141.
(58) (a) Baltes, T.; Garret-Flaudy, F.; Freitag, R. *J. Polym. Sci., Part A: Polym. Chem.* **1999**, *37*, 2977-2989. (b) Murray, M.; Rana, F.; Haq, I.; Cook, J.; Chowdhry, B. Z.; Snowden, M. J. *J. Chem. Soc., Chem. Commun.* **1994**, 1803-1804. (c) Snowden, M. J.; Chowdhry, B. Z.; Vincent, B.; Morris, G. E. *J. Chem. Soc., Faraday Trans.* **1996**, *92*, 5013-5016.
(59) Hennink, W. E.; van Nostrum, C. F. *Adv. Drug Deliv. Rev.* **2002**, *54*, 13-36.
(60) Llauro-Darricades, M. F.; Pichot, C.; Guillot, J.; Rios, L. G.; Cruz, M. A. E.; Guzman, C. *Polymer* **1986**, *27*, 889-898.
(61) Fujihara, H.; Yoshihara, M.; Maeshima, T. *J. Macromol. Sci. Chem.* **1980**, *14*, 867-877.
(62) (a) Charleux, B.; D'Agosto, F.; Delaittre, G. *Adv. Polym. Sci.* **2011**, *233*, 125-183. (b) Harada, A.; Kataoka, K. *Prog. Polym. Sci.* **2006**, *31*, 949-982.
(63) (a) Dirk, S. *Adv. Drug Deliv. Rev.* **2006**, *58*, 1655-1670. (b) Li, G.; Song, S.; Guo, L.; Ma, S. *J. Polym. Sci., Part A: Polym. Chem.* **2008**, *46*, 5028-5035.

Table 1. Experimental conditions and characteristics of the dispersion polymerizations of *N*,*N*-diethylacrylamide initiated by a SG1-terminated poly(sodium acrylate) macroalkoxyamine.[a]

Exp.	Symbol	Solids content[b]	T_{polym}	$[DEAAm]_0$	$[Comonomer]_0$	$[PAA\text{-}SG1]_0$	$[SG1]_0$	Final conv.	$DP_{n,th}$[c]	$D_{n,50°C}$ (σ)[d]	N_p	PTT[e]
		wt%	*°C*	*mol.L^{-1}*	*mol% based on monomers*	*mol.L$_{aq}^{-1}$*	*mol% based on PAA-SG1*			*nm*	*L^{-1}*	*°C*
1	●	19.9	120	1.57	-	7.3×10^{-3}	-	0.99	270	110 (0.22)	2.8×10^{17}	-
2	♦	19.9	112	1.57	-	7.3×10^{-3}	-	0.98	270	70 (0.09)	1.1×10^{18}	-
3	■	19.9	112	1.57	-	7.3×10^{-3}	5.0	0.99	270	70 (0.03)	1.1×10^{18}	-
4	▲	19.9	112	1.58	-	7.3×10^{-3}	9.8	0.90	250	70 (0.19)	1.0×10^{18}	32–34
5	●	19.8	112	1.55	-	3.6×10^{-3}	10.0	0.98	540	85 (0.20)	6.0×10^{17}	-
6	♦	19.9	112	1.59	-	1.08×10^{-2}	10.3	0.89	170	35 (0.02)	7.9×10^{18}	-
7	■	19.4	112	1.57	-	1.69×10^{-2}	10.4	0.96	115	30 (0.19)	1.3×10^{19}	-
8	▼	29.3	112	2.32	-	1.24×10^{-2}	9.7	0.92	250	65 (0.04)	1.9×10^{18}	-
9	●	39.0	112	3.08	-	1.94×10^{-2}	9.6	0.92	250	40 (0.04)	1.1×10^{19}	-
10	-	19.7 (26.9[f])	112	1.55	38.0 (51.2[g])	7.3×10^{-3}	9.6	0.70	-	95 (0.21)	4.2×10^{17}	-

[a] Pressure = 3 bars; $[Na_2CO_3]_0$ = 35 mM_{aq}; pH > 9.
[b] Solids content is actually theoretical and is used as a shortcut for monomer/water weight ratio
[c] Theoretical degree of polymerization of the PDEAAm block for the final sample (maximal conversion)
[d] Number-average diameter and dispersity factor (from Malvern Instrument) of the final sample determined by DLS at 50 °C without any cooling under PTT. It must be noted that all samples showed a thermoresponsive behavior during DLS measurements.
[e] Determined by HSDSC.
[f] Overall monomer content after styrene injection
[g] Recalculated by substracting DEAAm already converted at the time of the styrene injection

For Table of Contents use only

Synthesis by Nitroxide-Mediated Aqueous Dispersion Polymerization, Characterization, and Physical Core-Crosslinking of pH- and Thermoresponsive Dynamic Diblock Copolymer Micelles

Guillaume Delaittre, Maud Save, Marianne Gaborieau, Patrice Castignolles, Jutta Rieger, Bernadette Charleux**

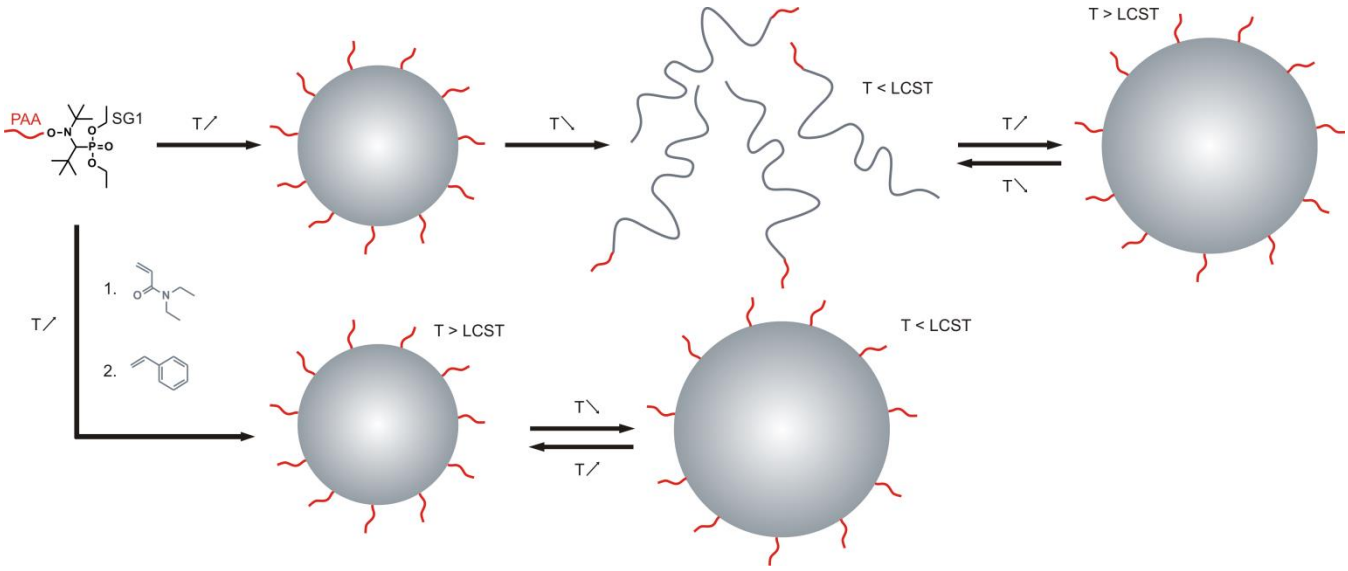

Supporting Information for:

Synthesis by Nitroxide-Mediated Aqueous Dispersion Polymerization, Characterization, and Physical Core-Crosslinking of pH- and Thermoresponsive Dynamic Diblock Copolymer Micelles

Guillaume Delaittre,[†] Maud Save,[‡] Marianne Gaborieau,[¤] Patrice Castignolles,[¶] Jutta Rieger,[§] Bernadette Charleux*[¥]

† Preparative Macromolecular Chemistry, Institut für Technische Chemie und Polymerchemie, Karlsruhe Institute of Technology (KIT), Engesserstr.18, 76128 Karlsruhe, Germany.

‡ IPREM Equipe de Physique et Chimie des Polymères, UMR 5254 CNRS, Université de Pau et des Pays de L'Adour, Hélioparc, 2 Avenue du Président Angot, 64053 Pau Cedex, France.

¤ University of Western Sydney, Nanoscale Organisation and Dynamics Group, School of Science and Health, Campbelltown Campus, Building 21, Locked Bag 1797, Penrith NSW 2751, Australia

¶ University of Western Sydney, School of Science and Health, Australian Centre for Research on Separation Science (ACROSS), Parramatta Campus, Locked Bag 1797, Penrith NSW 2751, Australia.

§ UPMC Univ. Paris 6, Sorbonne Universités and CNRS, Laboratoire de Chimie des Polymères, UMR 7610, 3 rue Galilée, 94200 Ivry, France.

¥ Université de Lyon, Univ Lyon 1, CPE Lyon, CNRS, UMR 5265, C2P2 (Chemistry, Catalysis, Polymers & Processes), Team LCPP Bat 308F, 43 Bd du 11 novembre 1918, 69616 Villeurbanne, France.

Mark-Houwink-Sakurada parameters of PMMA in DMF/LiBr

No Mark-Houwink-Sakurada parameters are available for PMMA in DMF/LiBr at 60 °C in the literature. A number of M_w and [η] values have however been determined in pure DMF at different temperatures ranging from 10 to 60 °C (see Table S1). We compared the values of

intrinsic viscosity and molecular weight. One set of value is a clear outlier (last line of Table S1).

Table S1. Viscosity properties (intrinsic viscosity, $[\eta]$, and weight-average molecular weight, M_w) of PMMA in DMF measured at different temperatures T.

M_w (g/mol)	$[\eta]$ (dL/g)	T (°C)	Determination method	Reference
82,600	0.297	25	Offline static light scattering and Ubelhode viscometer in dried DMF under nitrogen	[1]
124,000	0.39			
173,000	0.45			
202,000	0.517			
287,000	0.61			
360,000	0.77			
527,000	0.955			
1100,000	1.62			
17,500,000	7.7			
18,600,000	8.77			
22,700,000	9.62			
23,800,000	9.98			
17,500,000	7.7	25	Offline static light scattering and viscometer	[2]
18,600,000	8.77			
22,700,000	9.62			
23,800,000	9.98			
9,513,000	3.32	25	Offline static light scattering and Ubelhode viscometer	[3]
10,961,000	3.66			
12,175,000	3.981			
15,998,000	4.551			
15,923,000	4.657			
23,175,000	5.7676			
9,513,000	3.32			
64,368	0.233	60	?	Viscotek
714,000	0.887	10	Offline static light scattering and	[4]
606,000	0.813			

547,000	0.753		Ubelhode viscometer	
485,000	0.684			
319,000	0.561			
220,000	0.428			
87,000	0.255			
714,000	0.99	30		
606,000	0.894			
547,000	0.821			
485,000	0.729			
319,000	0.607			
220,000	0.465			
87,000	0.26			
714,000	1.041	50		
606,000	0.966			
547,000	0.872			
485,000	0.771			
319,000	0.635			
220,000	0.492			
87,000	0.274			
550,000	0.815	15	Offline static light scattering and Ubelhode viscometer	5
420,000	0.692			
300,000	0.533			
80,000	0.214			
550,000	0.89	25		
420,000	0.73			
300,000	0.567			
80,000	0.223			
550,000	0.919	35		
420,000	0.768			
300,000	0.6			
80,000	0.229			
550,000	0.979	45		
420,000	0.805			

300,000	0.624			
80,000	0.235			
420,000	0.837	55		
300,000	0.646			
80,000	0.249			
40,500	0.005	60	?+viscosimeter	[6]

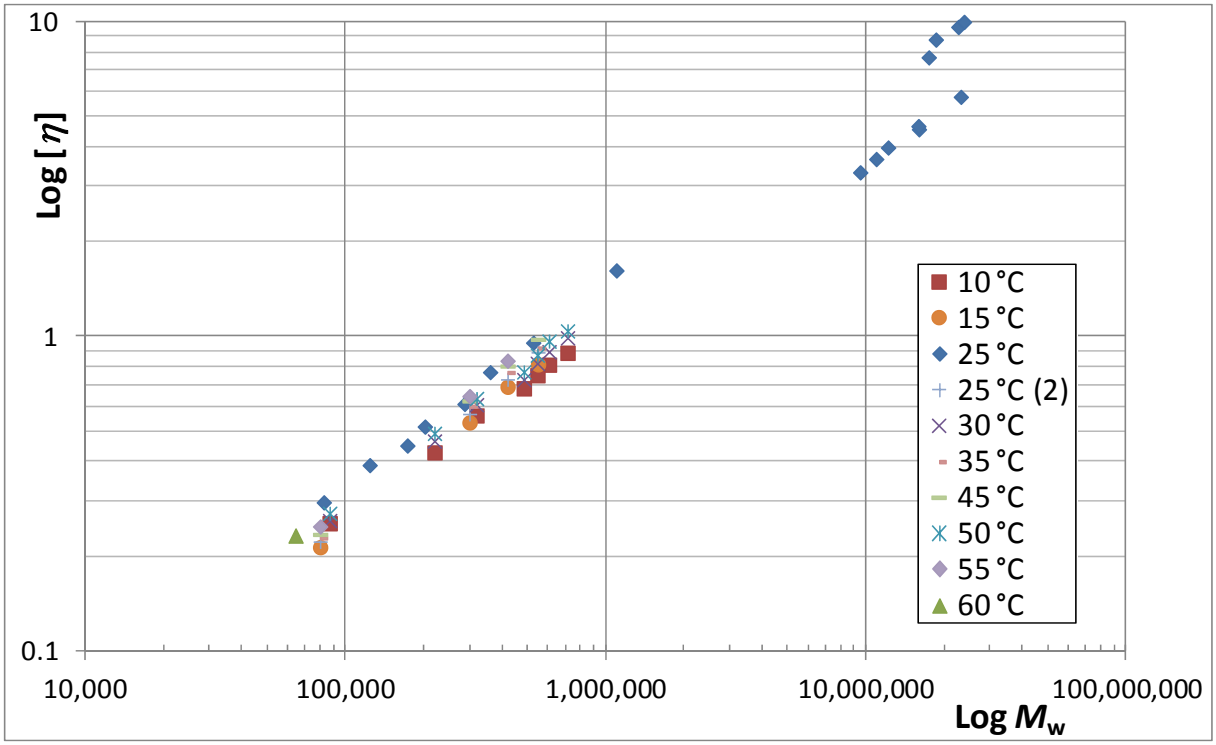

Figure S1. Mark-Houwink-Sakurada plot for PMMA in DMF measured at different temperatures (see references in Table S1 for the different literature values).

All other values given in the literature are consistent (see Figure S1). Values at 55 °C and 60 °C were plotted and fitted together (Figure S-2) to obtain the following equation:

$$\text{Log } [\eta] = 0.6961 \log M_w - 3.9979 \qquad (1)$$

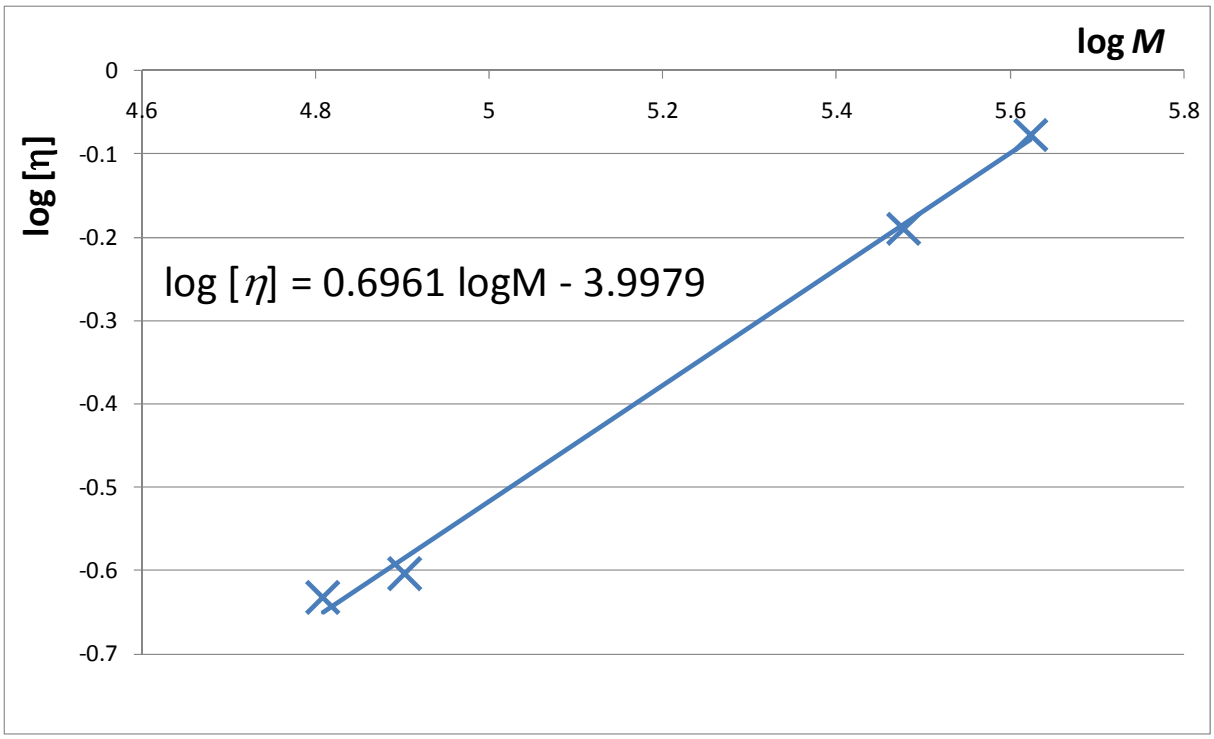

Figure S2. Mark-Houwink-Sakurada plot for PMMA in DMF measured at 55-60 °C.

Universal calibration in our SEC system

Polystyrene standards lead to a universal calibration significantly different from the PMMA one (Figure S3). Polystyrene has too low a polarity compared to the one of the stationary phase and eluents and likely adsorbs as already observed.[7] Polystyrene is certainly not separated by a size-exclusion mechanism with the Mixed C column in DMF. The universal calibration curve was thus built only with PMMA standards.

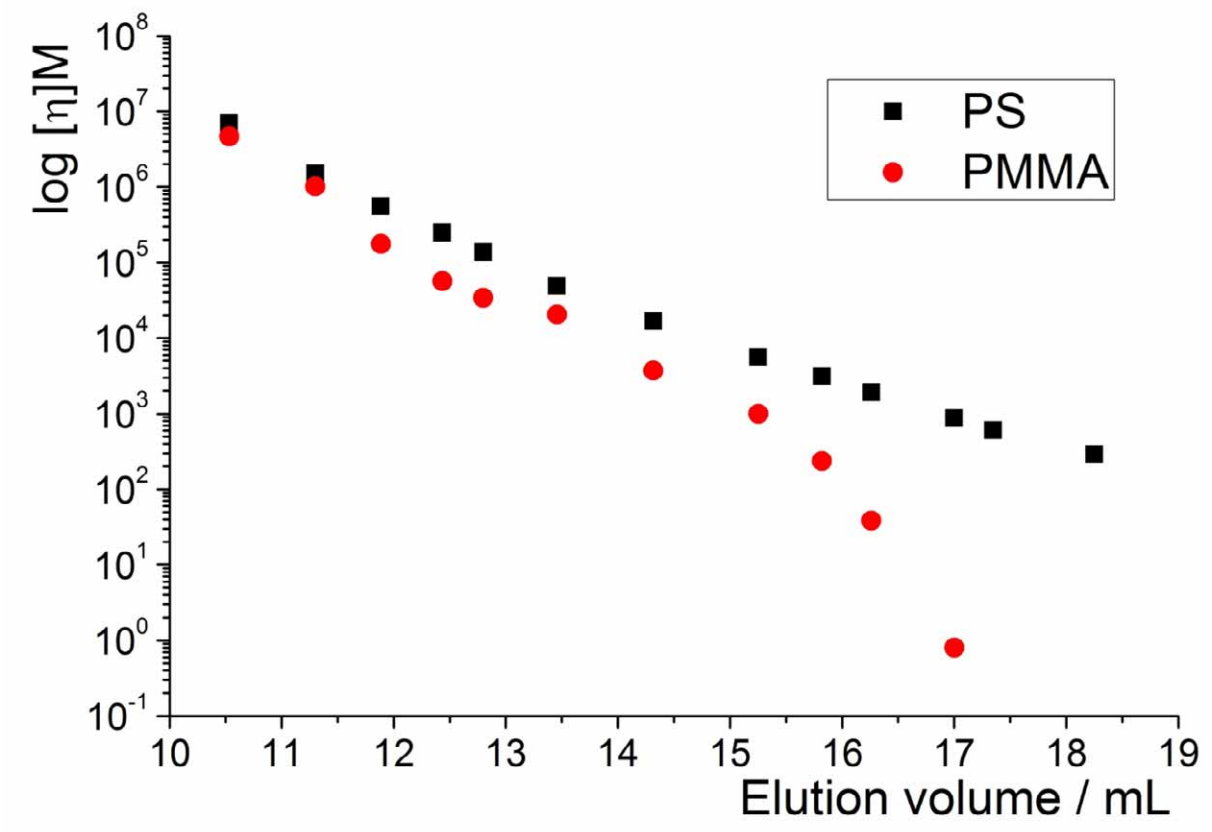

Figure S3. Comparison of the universal calibration curves obtained with polystyrene (black squares) and poly(methyl methacrylate) (red circles).

SEC Chromatograms

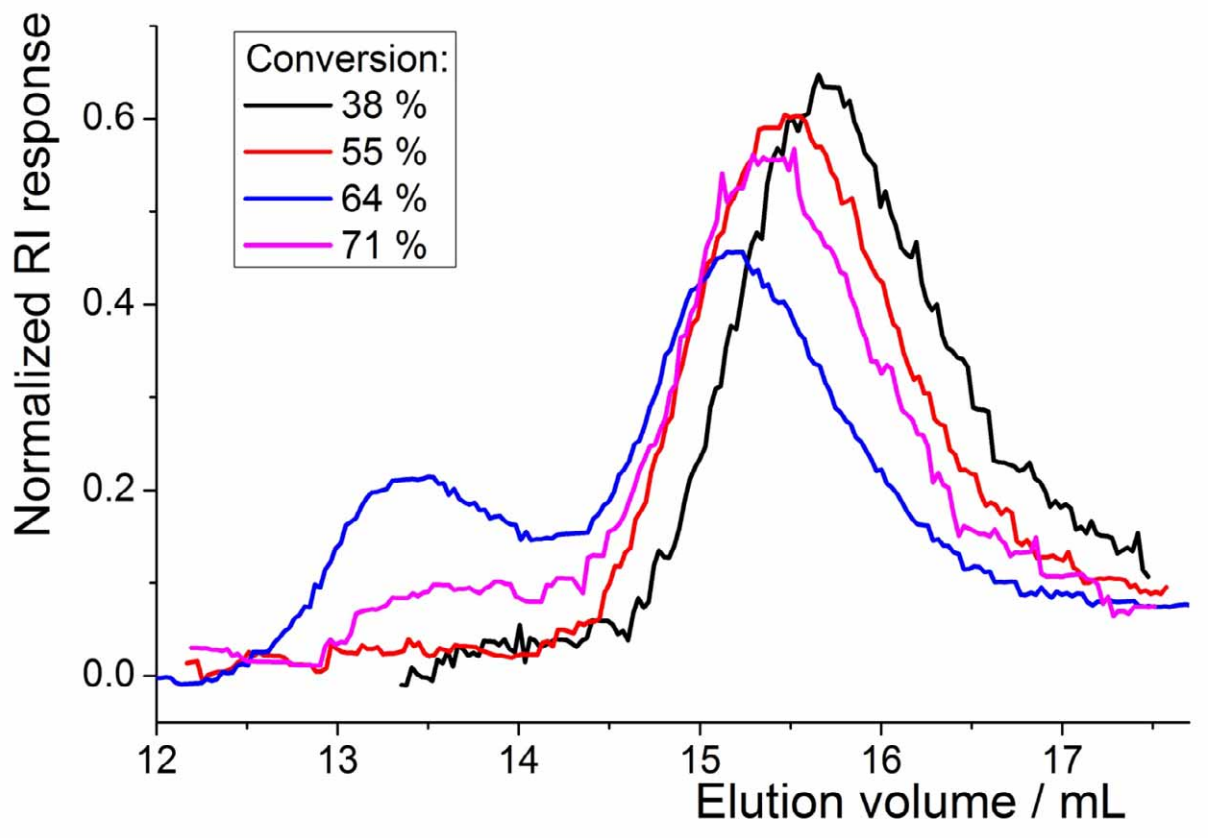

Figure S4. Chromatograms obtained by SEC/DMF of PAA-*b*-PDEAAm synthesized by dispersion polymerization of DEAAm initiated by PAA_{23}-SG1 at 112 °C (exp. 7).

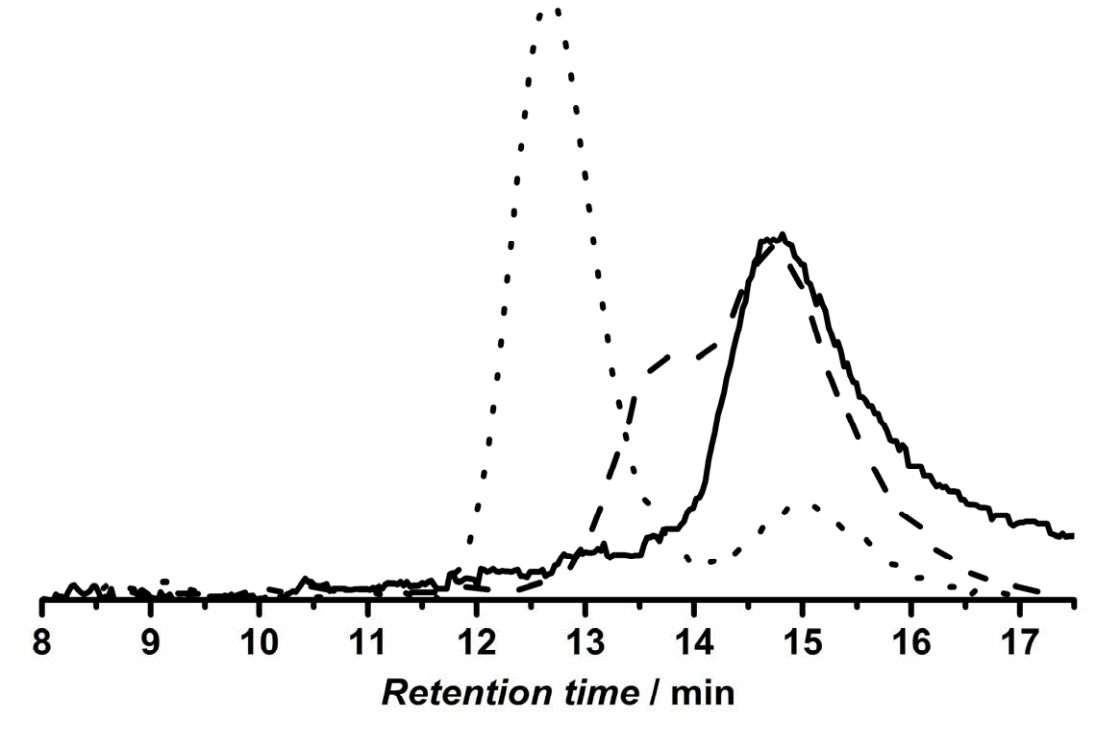

Figure S5. Chromatograms obtained by SEC/DMF of PAA-*b*-PDEAAm synthesized by dispersion polymerization of DEAAm initiated by PAA_{23}-SG1 after different treatments [acidification and drying on Mg_2SO_4 (dotted line); acidification and methylation (dashed line); and randomly obtained non-aggregated sample (solid line)].

Hydrodynamic volume distributions (HVDs)

HVDs can be determined from the raw bimodal refractometer signal, without deconvolution, using the equation below:[8]

$$w(\log V_h) = V_h W(V_h) = \left. \frac{S^*_{DRI}(t_{el})}{\frac{d \log V_h}{d\tilde{t}_{el}(V_h)}} \right|_{\tilde{t}_{cl}(V_h)=t_{cl}}$$

where V_h is the hydrodynamic volume, $w(\log V_h)$ is the SEC hydrodynamic volume distribution, $W(V_h)$ is the weight hydrodynamic volume distribution, $S^*_{DRI}(t_{el})$ is the refractometer signal at the elution time t_{el}, and $d\log V_h/dt_{el}(V_h)$ is the value of the derivative of the universal calibration curve at the hydrodynamic volume V_h.

HVDs are presented on Figures S6 and S7. Figure S7 shows that the aggregate peak represent a very small proportion of the total sample in terms of weight or number. However, this

weight distribution exhibits a low signal-to-noise ratio for the polymer peak and can thus not be used for comparison purposes.

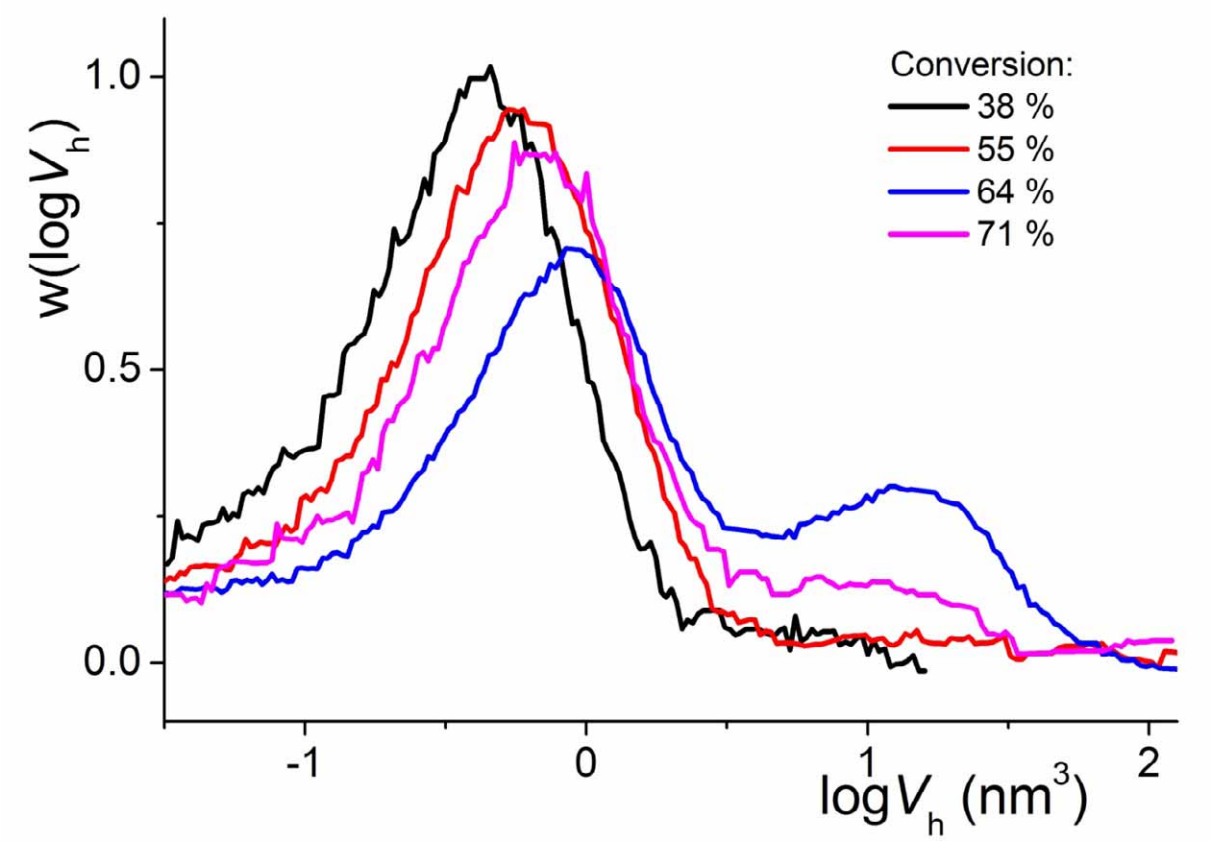

Figure S6. SEC hydrodynamic volume distributions (w(log V_h)) calculated from the chromatograms presented in Figure S4 (exp. 7).

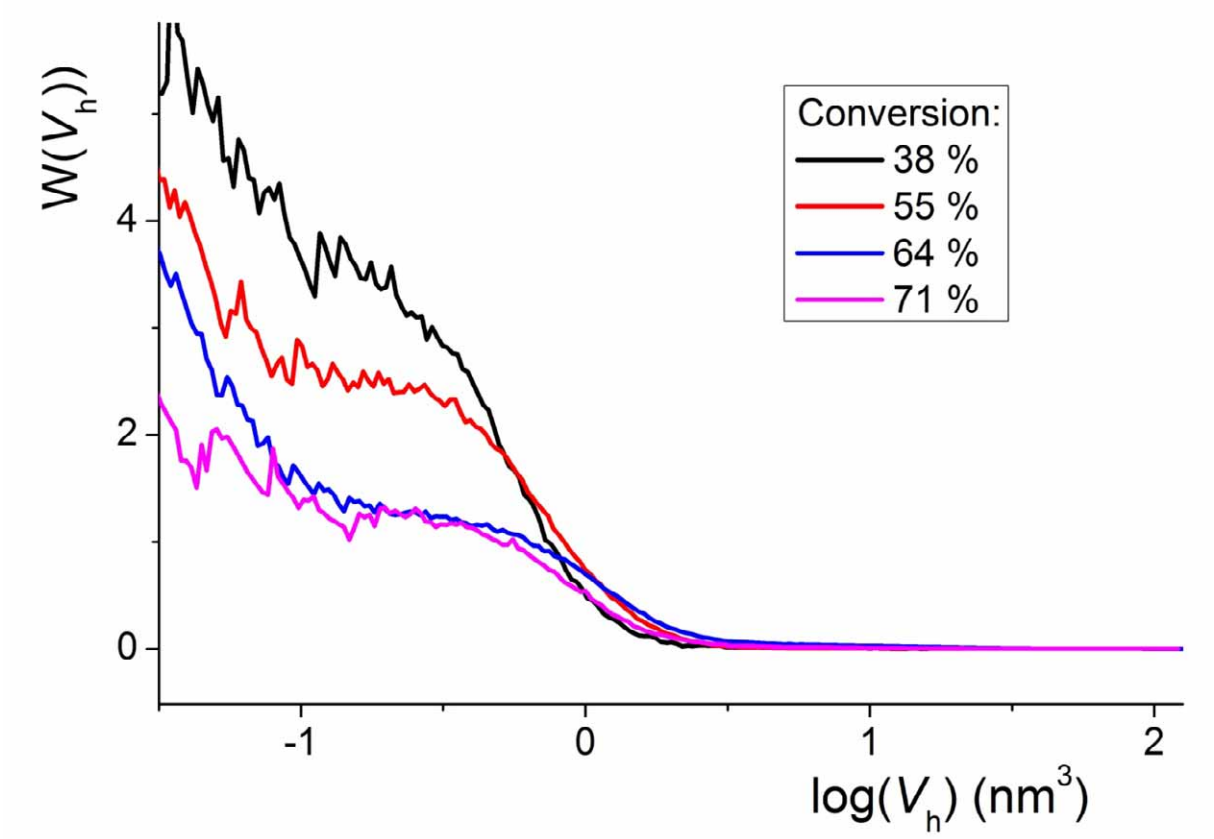

Figure S7. Weight hydrodynamic volume distributions (W(V_h)) calculated from the SEC distributions presented in Figure S4 (exp. 7).

Deconvolution

The deconvolution of the data corresponding to Figure S4, S6, and S7 is presented on Figure S8 in the case of Gaussian functions. This deconvolution is easily performed using the "multiple peaks" function of the software Origin (OriginLab). The sum of the two deconvoluted peaks poorly represents the original distribution, especially in terms of baseline. The problem is also observed when the deconvolution is done on the chromatogram (data not shown).

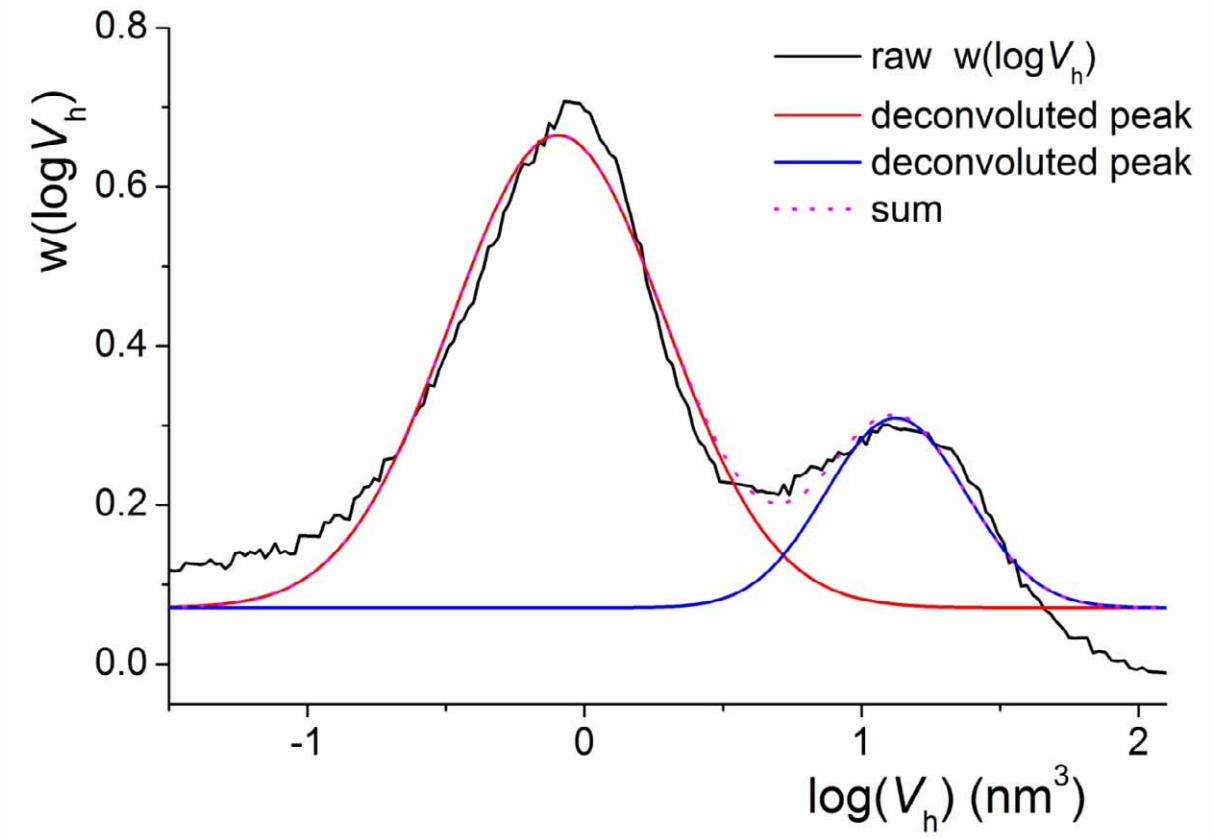

Figure S8. Deconvolution of Figure S4 (64 % conversion) using multiple Gaussian peaks.

The first issue with the deconvolution is that part of the low molecular weight tail is missing. Incomplete separation of oligomers and system peaks is a common limitation of SEC, especially recognized to lead to poor accuracy of number-average molecular weights (M_n)[9,10]. The fact that the low-molecular weight tail is missing is also an issue for the deconvolution. To obtain the correct baseline after deconvolution, we have substituted system peaks eluting after the calibration curve (PMMA-equivalent molecular weight inferior to 200 g/mol) by a perfect baseline: 200 points have been added for elution volumes between 18 and 20 mL with a RI response of 0. The large error in baseline is then significantly reduced. The sum of the two deconvoluted peaks still fits poorly the overall hydrodynamic distribution (Figure S9) or chromatogram (data not shown).

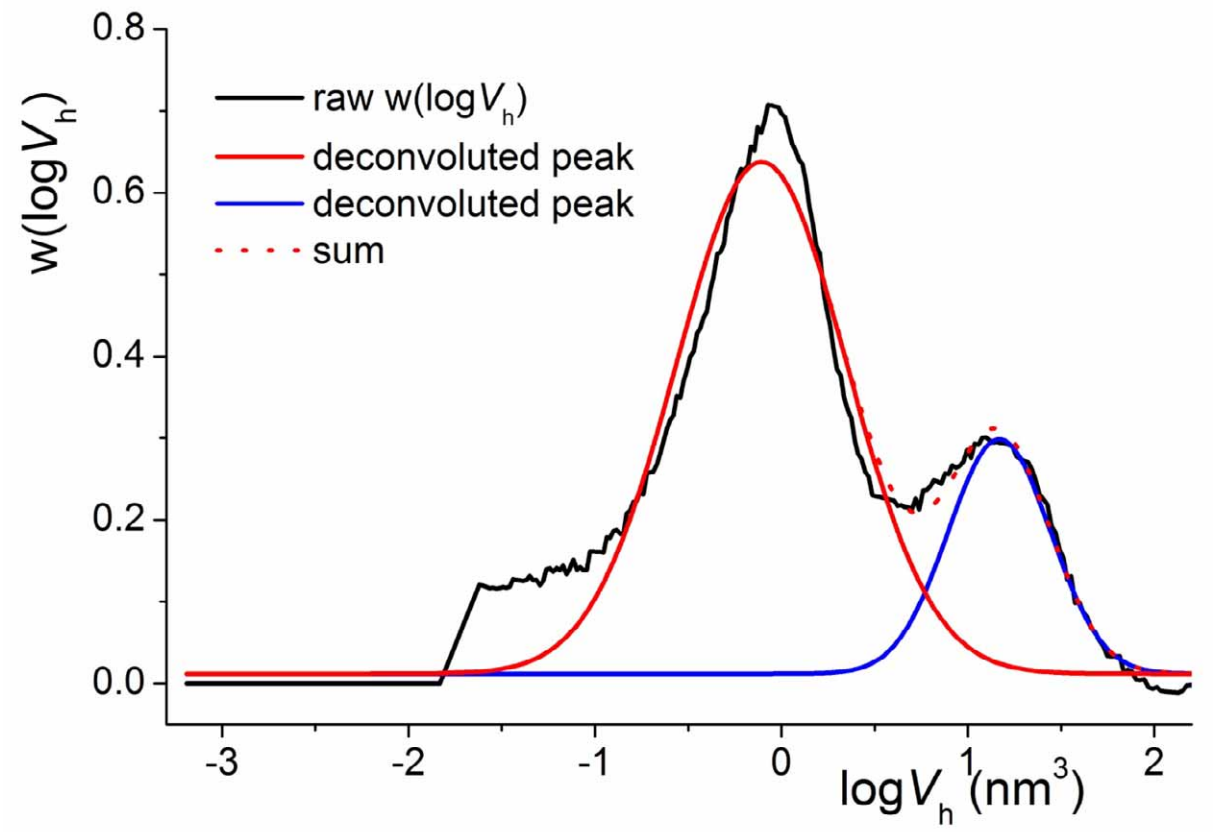

Figure S9. Same deconvolution as Figure S8 after addition of 200 "0" points.

These data were then deconvoluted using exponentially modified Gaussians. The software PeakFit (Jandel) was used for that purpose. The sum of the two deconvoluted peaks is clearly fitting better by simple visual inspection of both the chromatogram (Figure S-9) and the hydrodynamic volume distribution w(log V_h) (Figure S-10). The fit leads to visually the same results with or without addition of "zero" and the addition was thus not performed using PeakFit (data not shown).

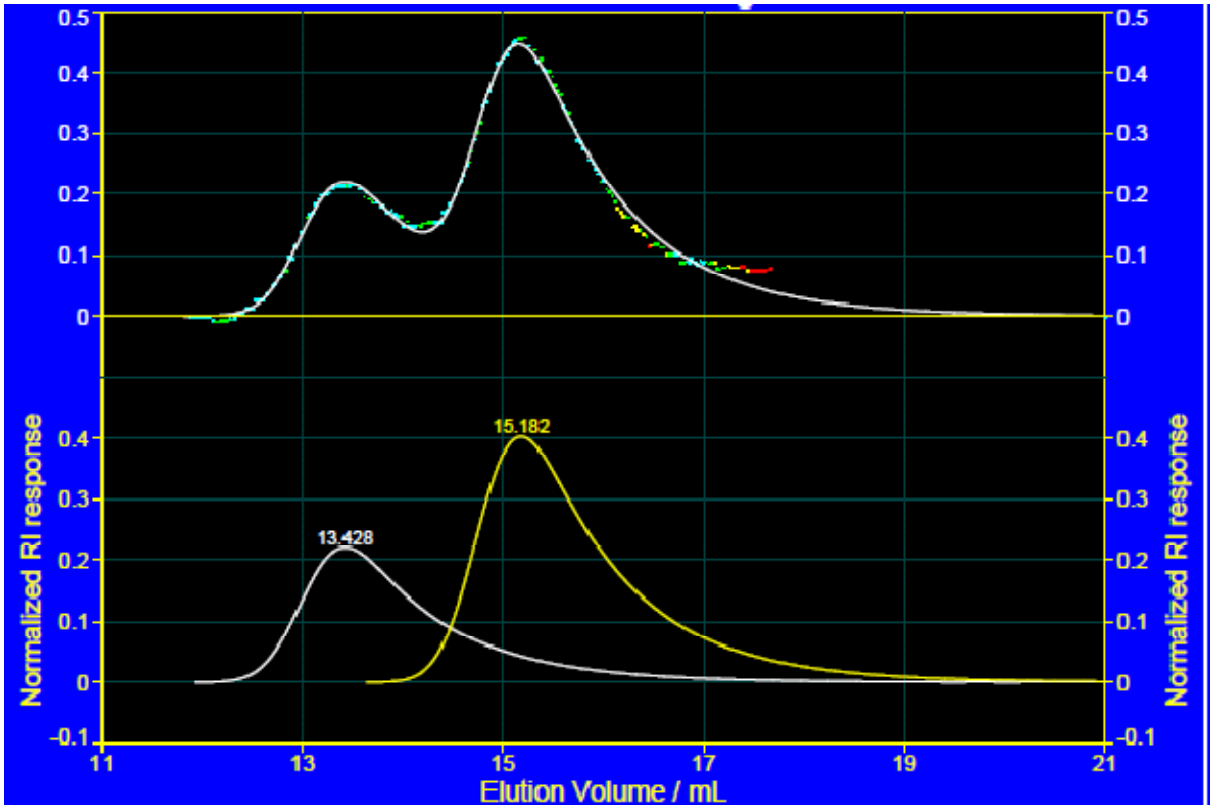

Figure S10. Deconvolution of the chromatogram presented in Figure S4 (conversion 64 %) using PeakFit: deconvoluted peaks (bottom) and sum (top, full line) compared to raw chromatogram (top, dotted line).

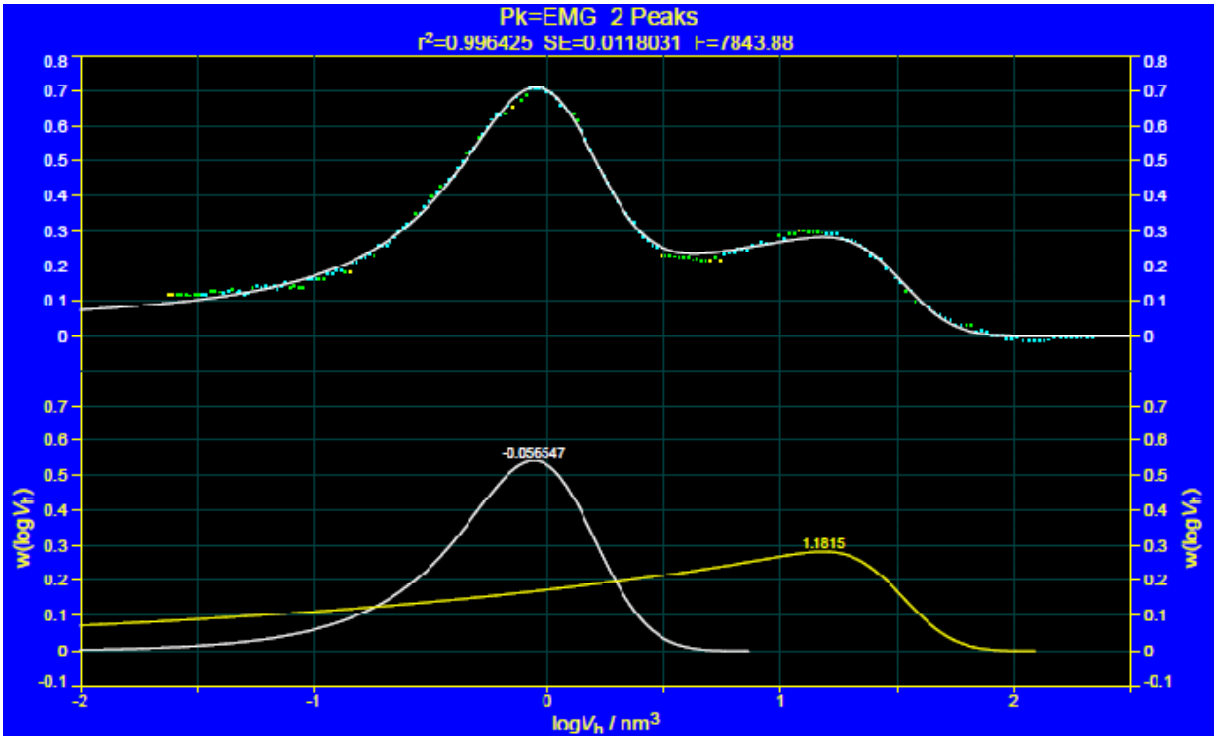

Figure S11. Deconvolution of the hydrodynamic volume distribution presented in Figure S6 (64% conversion) using PeakFit: deconvoluted peaks (bottom) and sum (top, full line) compared to raw chromatogram (top, dotted line). Note that this distribution corresponds to the chromatogram presented on Figure S10.

It is important to note that the deconvolution of the hydrodynamic volume distribution leads in the oligomers range to a higher proportion of aggregates than free polymer chains. This is physically impossible. Furthermore, the two types of deconvolutions lead to different results when the hydrodynamic volume distributions are compared (Figure S12). The deconvolutions were thus performed on the raw chromatograms before calculating the hydrodynamic volume distribution corresponding to the polymer peak.

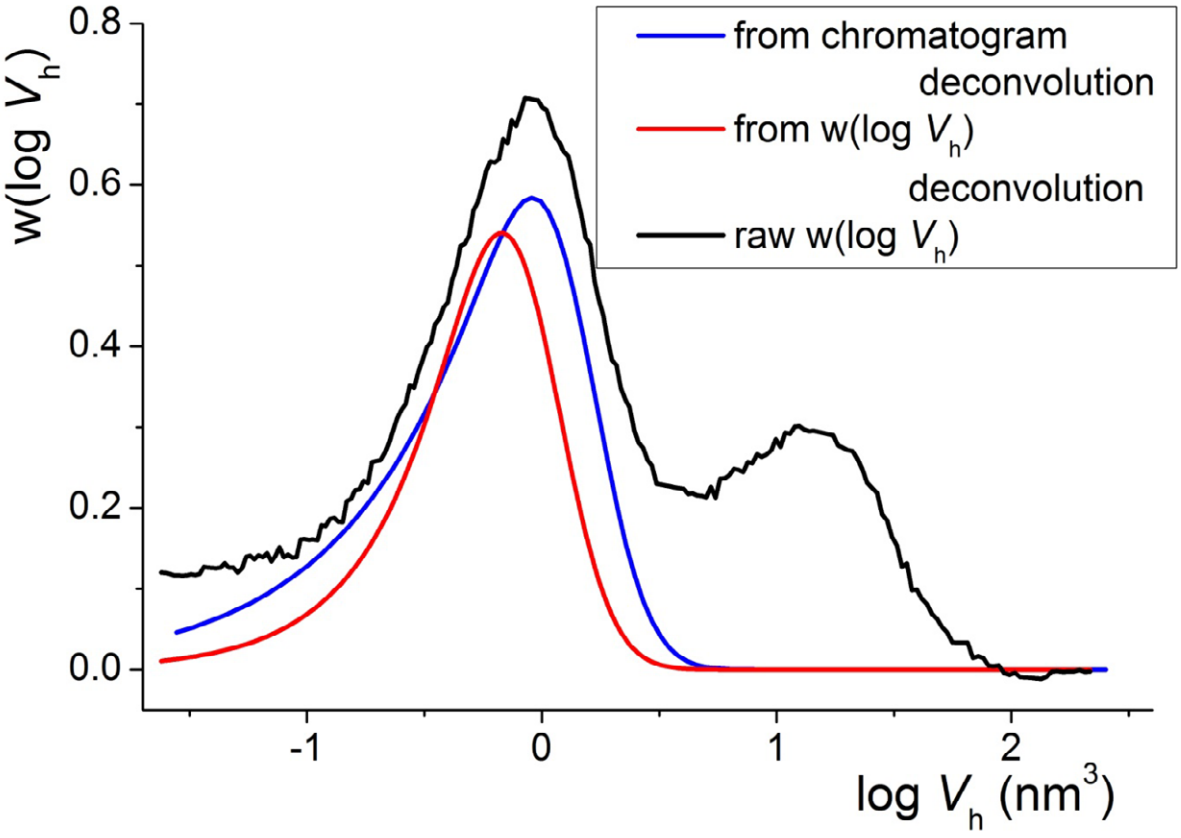

Figure S12. Comparison of the raw w(log Vh) distribution (black line) with w(log Vh) corresponding to the polymeric unimers obtained from deconvolution of the w(log Vh) (red line) or from deconvolution of the chromatogram (blue line).

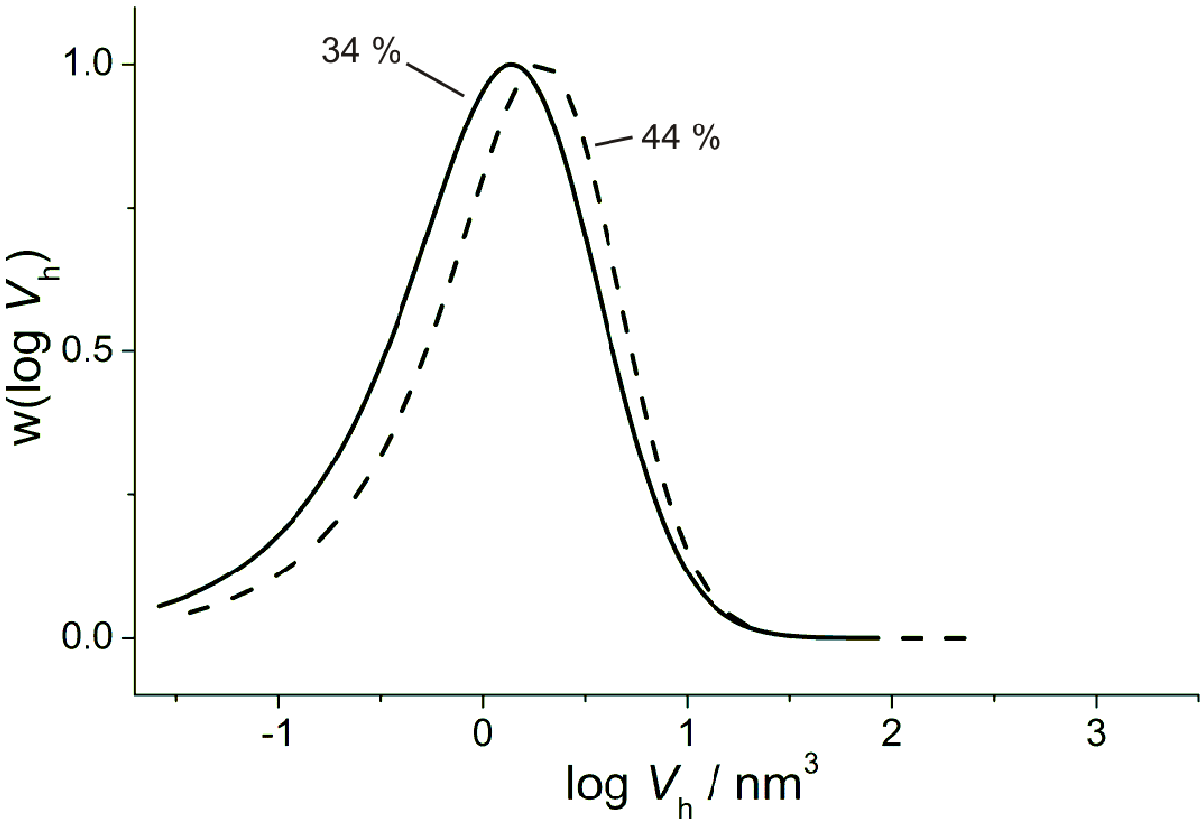

Figure S13. Overlay of hydrodynamic volume distributions at two monomer conversions for the dispersion polymerization of DEAAm initiated by PAA_{23}-SG1 at 112 °C, $[PAA\text{-}SG1]_0$ = 7.3×10^{-3} mol L_{aq}^{-1}, 20 wt.% solids, and r = 0.05 (Exp. 3).

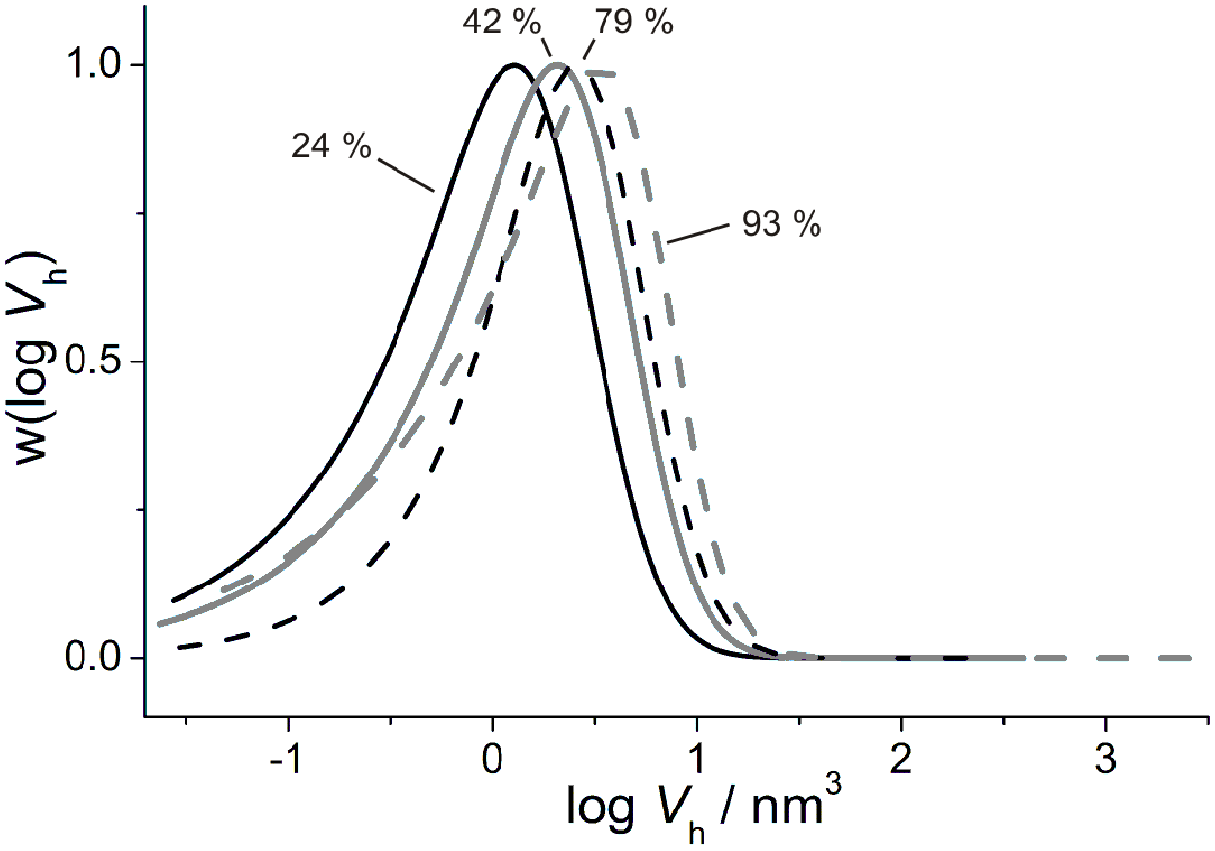

Figure S14. Overlay of hydrodynamic volume distributions at different monomer conversions for the dispersion/emulsion polymerization of DEAAm and styrene initiated by PAA_{23}-SG1 at 112 °C, 30 wt.% solids, $[PAA\text{-}SG1]_0 = 1.24 \times 10^{-2}$ mol L_{aq}^{-1}, and r = 0.10 (Exp. 8).

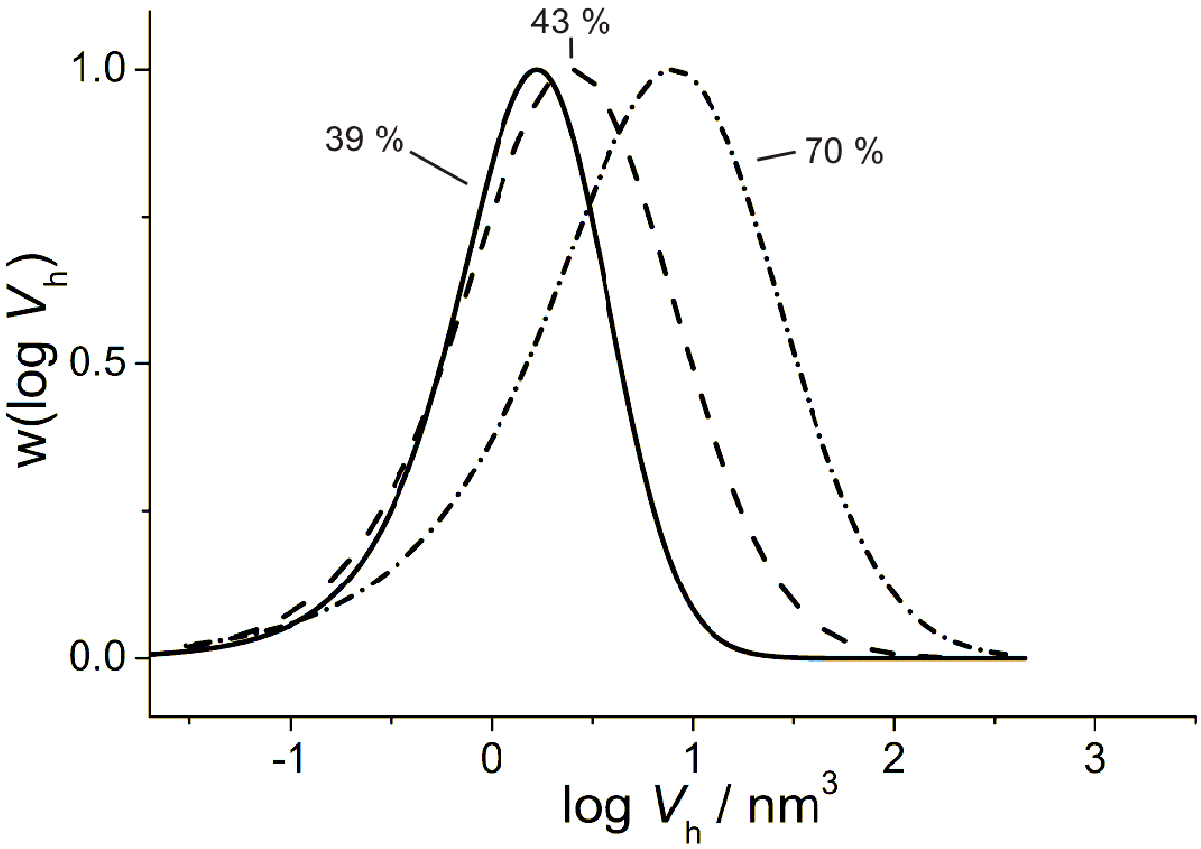

Figure S15. Overlay of hydrodynamic volume distributions at different monomer conversions for the dispersion/emulsion polymerization of DEAAm and styrene initiated by PAA_{24}-SG1 at 112 °C, 30 wt.% solids, $[PAA\text{-}SG1]_0 = 7.3 \times 10^{-3}$ mol L_{aq}^{-1}, and r = 0.10 (Exp. 10).

Correlation between particle size and theoretical degree of polymerization of the PDEAAm block

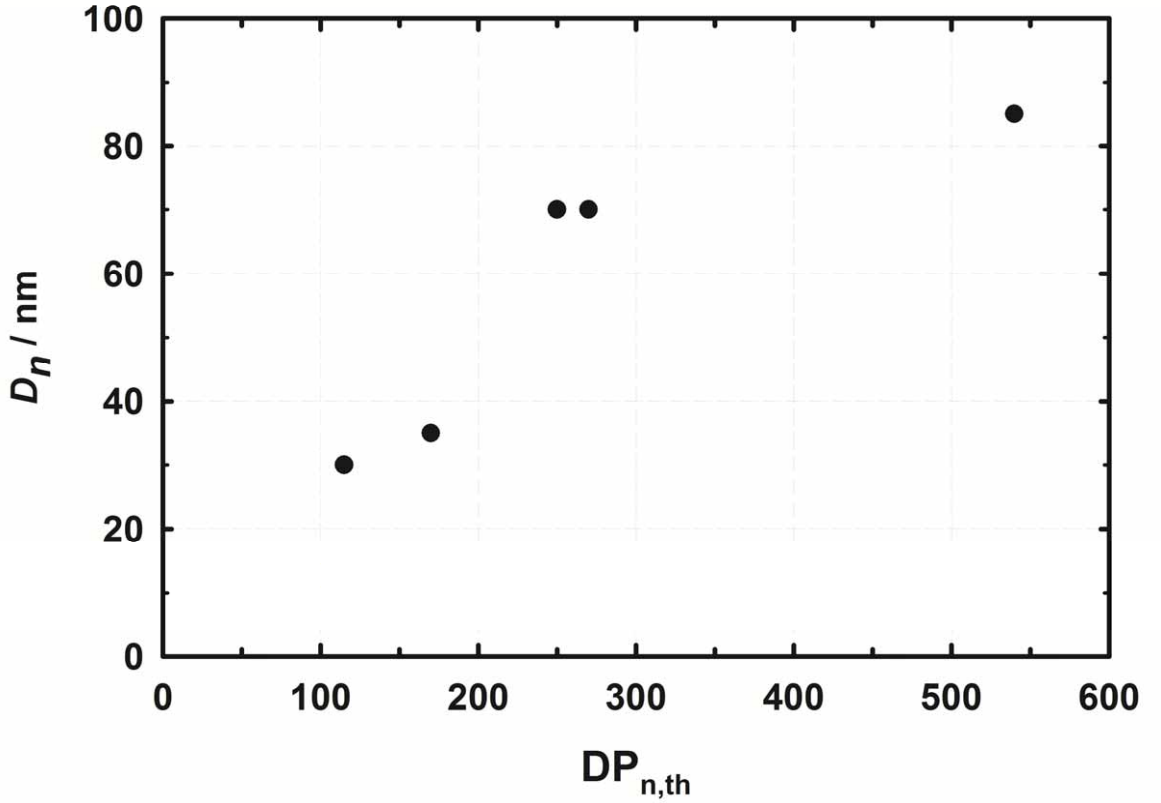

Figure S16. Observed number-average hydrodynamic diameter of the final samples (solids content ~ 20 wt%, exps. 2–7) vs. theoretical degree of polymerization of the PDEAAm block at final conversion.

High-sensitivity scanning differential calorimetry additional data

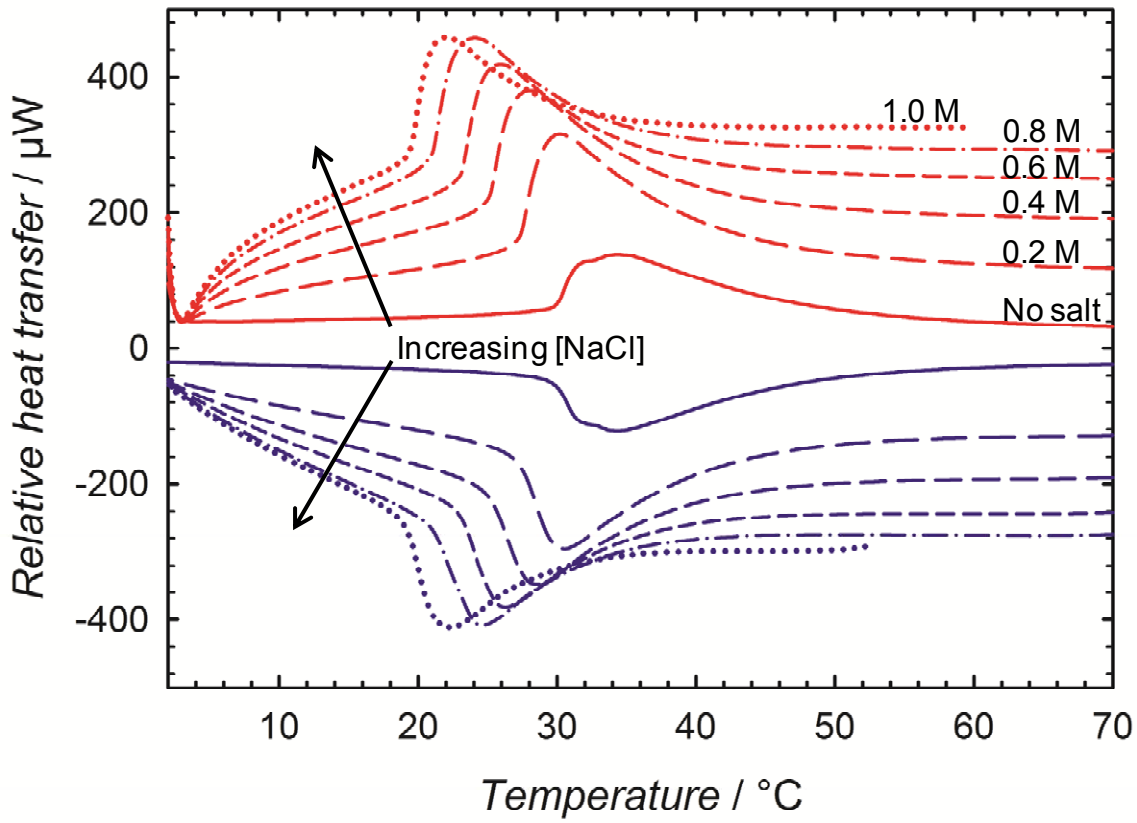

Figure S17. Heat transfer measured by HSDSC on a dialyzed solution of PAA-*b*-PDEAAm copolymers (5 g L^{-1}) at different NaCl concentrations (pH = 6.5). The red curves represent the heating endothermic scans and the blue ones represent the cooling exothermic scans. Heating and cooling rates were 1 °C min^{-1}.

Copolymerization parameters of DEAAm and styrene (S) (physical crosslinking experiment)

To estimate the copolymerization behavior of styrene with DEAAm in exp. 10, we referred to the closest copolymerization system previously published, *i.e.*, copolymerization of styrene with DMAAm in ethanol (the closest solvent to water in the report) at 80 °C (the highest temperature in the report).[11] The reported reactivity ratios were the following: r_S = 1.00 and r_{DMAAm} = 0.19.

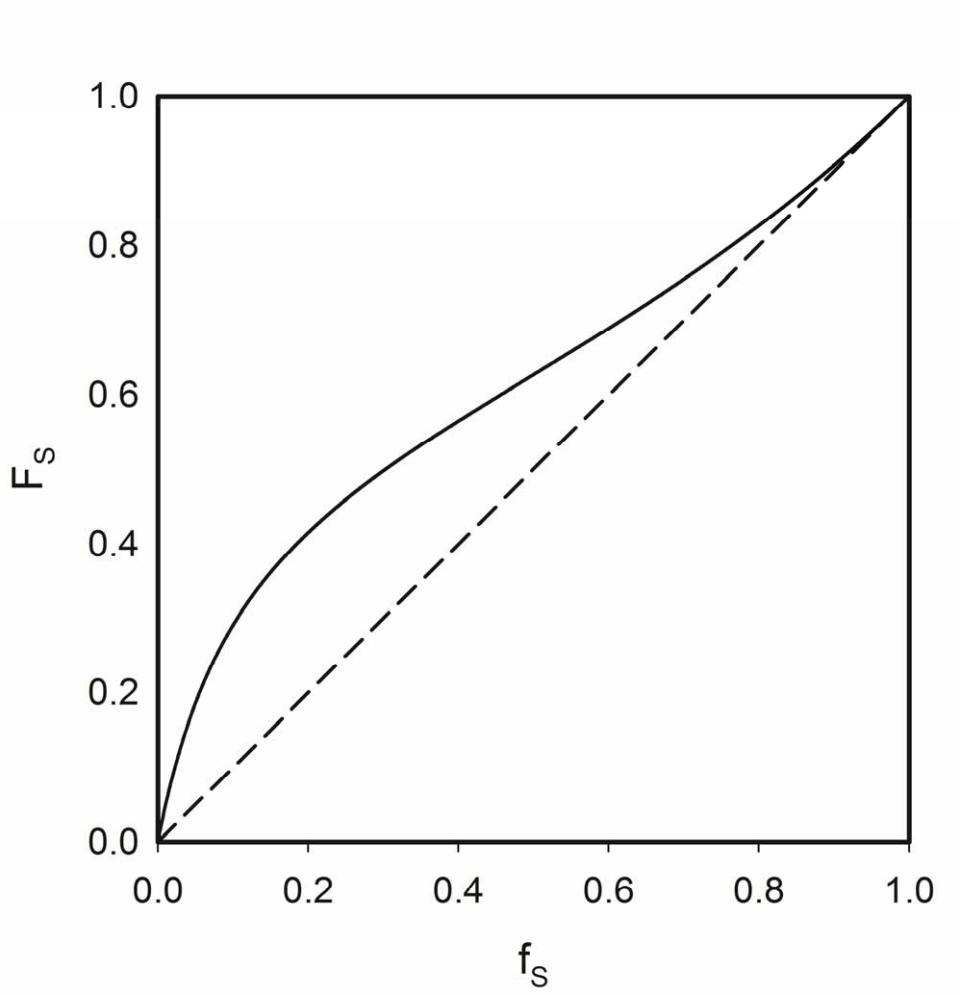

Figure S18. Evolution of the theoretical molar fraction of styrene (S) in a S/DMAAm copolymer vs the molar fraction of S in the comonomer mixture with r_S = 1.00 and r_{DMAAm} = 0.19 (polymerization at 80 °C in ethanol).[11]

References

(1) Kossler, I.; Netopilik, M.; Schulz, G.; Gnauck, R. *Polymer Bulletin* **1982**, *7*, 597-598.

(2) Ioan, S.; Bercea, M.; Ioan, C.; Simionescu, B. C. *Eur. Polym. J.* **1995**, *31*, 85-89.

(3) Bercea, M.; Ioan, C.; Morariu, S.; Ioan, S.; Simionescu, B. C. *Polym.-Plast. Technol. Eng.* **1998**, *37*, 285-294.

(4) Kambe, Y. S. *J. Phys. Chem.* **1968**, *72*, 4104-4110.

(5) Cesteros, L. C.; Katime, I. *Eur. Polym. J.* **1984**, *20*, 237-240.

(6) Tewari, N.; Srivastava, A. K. *Macromolecules* **1992**, *25*, 1013-1016.

(7) Temyanko, E.; Russo, P. S.; Ricks, H. *Macromolecules* **2001**, *34*, 582-586.

(8) Gaborieau, M.; Gilbert, R. G.; Gray-Weale, A.; Hernandez, J. M.; Castignolles, P. *Macromol. Theory Simul.* **2007**, *16*, 13-28.

(9) Berek, D.; Bruessau, R.; Lilge, D.; Mingozzi, T.; Podzimek, S.; Robert, E. In *IUPAC congress/ general assembly*; http://old.iupac.org/projects/posters01/berek01.pdf, Ed., July 2001.

(10) Bruessau, R. J. *Macromol. Symp.* **1996**, *110*, 15-32.

(11) Fujihara, H.; Yoshihara, M.; Maeshima, T. *J. Macromol. Sci. Chem.* **1980**, *14*, 867-877.